

Evaluating
emissions of
biogenic
bromocarbons

R. Hossaini et al.

This discussion paper is/has been under review for the journal Atmospheric Chemistry and Physics (ACP). Please refer to the corresponding final paper in ACP if available.

Evaluating global emission inventories of biogenic bromocarbons

R. Hossaini¹, H. Mantle¹, M. P. Chipperfield¹, S. A. Montzka², P. Hamer³, F. Ziska⁴, B. Quack⁴, K. Krüger⁴, S. Tegtmeier⁴, E. Atlas⁵, S. Sala⁶, A. Engel⁶, H. Bönisch⁶, T. Keber⁶, D. Oram⁷, G. Mills⁷, C. Ordóñez⁸, A. Saiz-Lopez⁹, N. Warwick¹⁰, Q. Liang¹¹, W. Feng¹, F. Moore², B. R. Miller², V. Marécal³, N. A. D. Richards¹, M. Dorf¹², and K. Pfeilsticker¹²

¹Institute for Climate and Atmospheric Science (ICAS), School of Earth and Environment, University of Leeds, Leeds, UK

²National Oceanic and Atmospheric Administration, Boulder, USA

³Centre National de Recherches Météorologiques-Groupe d'étude de l'Atmosphère Météorologique, Météo-France and CNRS, Toulouse, France

⁴GEOMAR Helmholtz Centre for Ocean Research Kiel, Kiel, Germany

⁵Rosenstiel School of Marine and Atmospheric Science, University of Miami, Miami, USA

⁶Institute for Atmospheric and Environmental Sciences, Universität Frankfurt/Main, Germany

⁷School of Environmental Sciences, University of East Anglia, Norwich, UK

⁸Met Office, Exeter, UK

⁹Atmospheric Chemistry and Climate Group, Institute for Physical Chemistry Rocasolano, CSIC, Madrid, Spain

Title Page

Abstract

Introduction

Conclusions

References

Tables

Figures

⏪

⏩

◀

▶

Back

Close

Full Screen / Esc

Printer-friendly Version

Interactive Discussion

¹⁰National Centre for Atmospheric Science (NCAS), University of Cambridge, Cambridge, UK

¹¹Universities Space Research Association, GESTAR, Columbia, Maryland, USA

¹²Institute for Environmental Physics, University of Heidelberg, Heidelberg, Germany

Received: 9 April 2013 – Accepted: 22 April 2013 – Published: 14 May 2013

Correspondence to: R. Hossaini (r.hossaini@see.leeds.ac.uk)

Published by Copernicus Publications on behalf of the European Geosciences Union.

**Evaluating
emissions of
biogenic
bromocarbons**

R. Hossaini et al.

Title Page

Abstract

Introduction

Conclusions

References

Tables

Figures

◀

▶

◀

▶

Back

Close

Full Screen / Esc

Printer-friendly Version

Interactive Discussion

Abstract

Emissions of halogenated very short-lived substances (VSLs) are poorly constrained. However, their inclusion in global models is required to simulate a realistic inorganic bromine (Br_y) loading in both the troposphere, where bromine chemistry perturbs global oxidizing capacity, and in the stratosphere, where it is a major sink for ozone (O_3). We have performed simulations using a 3-D chemical transport model (CTM) including three *top-down* and a single *bottom-up* derived emission inventory of the major brominated VSLs bromoform (CHBr_3) and dibromomethane (CH_2Br_2). We perform the first concerted evaluation of these inventories, comparing both the magnitude and spatial distribution of emissions. For a quantitative evaluation of each inventory, model output is compared with independent long-term observations at National Oceanic and Atmospheric Administration (NOAA) ground-based stations and with aircraft observations made during the NSF HIAPER Pole-to-Pole Observations (HIPPO) project. For CHBr_3 , the mean absolute deviation between model and surface observation ranges from 0.22 (38%) to 0.78 (115%) parts per trillion (ppt) in the tropics, depending on emission inventory. For CH_2Br_2 , the range is 0.17 (24%) to 1.25 (167%) ppt. We also use aircraft observations made during the 2011 “Stratospheric Ozone: Halogen Impacts in a Varying Atmosphere” (SHIVA) campaign, in the tropical West Pacific. Here, the performance of the various inventories also varies significantly, but overall the CTM is able to reproduce observed CHBr_3 well in the free troposphere using an inventory based on observed sea-to-air fluxes. Finally, we identify the range of uncertainty associated with these VSLs emission inventories on stratospheric bromine loading due to VSLs ($\text{Br}_y^{\text{VSLs}}$). Our simulations show $\text{Br}_y^{\text{VSLs}}$ ranges from ~ 4.0 to 8.0 ppt depending on the inventory. We report an optimised estimate at the lower end of this range (~ 4 ppt) based on combining the CHBr_3 and CH_2Br_2 inventories which give best agreement with the compilation of observations in the tropics.

Evaluating emissions of biogenic bromocarbons

R. Hossaini et al.

Title Page

Abstract

Introduction

Conclusions

References

Tables

Figures



Back

Close

Full Screen / Esc

Printer-friendly Version

Interactive Discussion



1 Introduction

On regional to global scales, bromine (Br) chemistry plays an important role in atmospheric composition. In the stratosphere, through coupling with analogous chlorine radicals, active bromine ($\text{Br}_x = \text{Br} + \text{BrO}$) takes part in catalytic cycles (e.g. BrO-CIO) which cause large seasonal ozone (O_3) loss during polar spring (e.g. Solomon, 1999, and references therein). At mid-latitudes, a cycle involving hydroperoxyl radicals (HO_2) (e.g., Lary, 1996) is also significant, particularly during periods of elevated stratospheric aerosol when heterogeneous halogen activation is enhanced (Salawitch et al., 2005; Feng et al., 2007). Reduced column O_3 increases the transmission of potentially harmful ultraviolet (UV) radiation to the surface, in addition to impacting surface temperature and climate both directly and indirectly (e.g., WMO, 2011, and references therein).

In the troposphere, where understanding of halogen impacts is evolving rapidly (e.g., Saiz-Lopez and Von Glasow, 2012), Br-mediated O_3 loss is also significant (Von Glasow et al., 2004; Yang et al., 2005), such as in the marine boundary layer (MBL) (e.g., Read et al., 2008) where biogenic emissions of halogenated species can be large (e.g., Carpenter and Liss, 2000; Quack and Wallace, 2003). Modelling work has also highlighted the importance of halogen-driven O_3 loss in the mid-upper troposphere (Saiz-Lopez et al., 2012). Through reactions involving HO_x (OH and HO_2) and NO_x (NO and NO_2), bromine chemistry may indirectly perturb oxidizing capacity and thus impact the lifetime of greenhouse gases (GHGs) such as methane (CH_4) (e.g., Lary and Toumi, 1997). Bromine chemistry may also impact other climate-relevant species; e.g. bromine monoxide (BrO) is a significant sink for dimethyl sulphide (DMS) – a precursor for cloud condensation nuclei (CCN) (Breider et al., 2010).

Sources of organic bromine include anthropogenic emissions of long-lived halons (e.g. CBrF_3 , Halon 1301) and also methyl bromide (CH_3Br), whose emissions are mostly biogenic (> 70%) (e.g., WMO, 2011). As their production is regulated under the Montreal Protocol (and amendments), the total tropospheric bromine burden from

ACPD

13, 12485–12539, 2013

Evaluating emissions of biogenic bromocarbons

R. Hossaini et al.

Title Page

Abstract

Introduction

Conclusions

References

Tables

Figures

⏪

⏩

◀

▶

Back

Close

Full Screen / Esc

Printer-friendly Version

Interactive Discussion

Evaluating emissions of biogenic bromocarbons

R. Hossaini et al.

Title Page

Abstract

Introduction

Conclusions

References

Tables

Figures

⏪

⏩

◀

▶

Back

Close

Full Screen / Esc

Printer-friendly Version

Interactive Discussion



these gases is now declining, from a peak observed towards the end of the 20th century (Montzka et al., 2003). Given their long tropospheric lifetimes, these gases are a relatively minor source of total inorganic bromine (Br_y) below the tropopause. However, in the stratosphere they account for $\sim 75\%$ of the total Br_y budget. The remainder is thought to arise from so-called very short-lived substances (VSLs) of predominately natural oceanic origin (e.g., Sturges et al., 2000; Pfeilsticker et al., 2000). In recent years, both observational (e.g., Sioris et al., 2006; Dorf et al., 2006, 2008; Salawitch et al., 2010; Brinckmann et al., 2012) and modelling (e.g., Schofield et al., 2011; Hossaini et al., 2012b; Tegtmeier et al., 2012; Aschmann and Sinnhuber, 2013) studies have constrained their contribution to stratospheric Br_y ($\text{Br}_y^{\text{VSLs}}$) – currently estimated at 1–8 parts per trillion (ppt) (Montzka et al., 2011).

The most abundant Br-containing VSLs are bromoform (CHBr_3) and dibromomethane (CH_2Br_2) with mean MBL mixing ratios of ~ 1.1 and 1.5 ppt. As their nominal surface lifetimes are short (~ 26 and 120 days, assuming $[\text{OH}] = 1 \times 10^6$ molecules cm^{-3} and a global/seasonal mean photolysis rate), and their emissions exhibit significant spatial/temporal inhomogeneity, tropospheric gradients can be large (Montzka et al., 2011). Localised *hot spots*, where emissions are relatively strong, have been identified; for example Mace Head (Ireland) (e.g., Carpenter et al., 2005). At present, the total global source strength of these VSLs are poorly constrained and range from $430\text{--}1400$ $\text{Gg Br}_y \text{yr}^{-1}$ and $57\text{--}280$ $\text{Gg Br}_y \text{yr}^{-1}$ for CHBr_3 and CH_2Br_2 (Montzka et al., 2011). For global-scale models, a sound treatment of the magnitude and spatial distribution of VSLs emissions is required in order to simulate a reasonable Br_y budget in both the troposphere and the stratosphere. As recent chemistry-climate model (CCM) studies suggest $\text{Br}_y^{\text{VSLs}}$ in the lower stratosphere may increase in response to climate change (Dessens et al., 2009; Hossaini et al., 2012a), validation of VSLs emission inventories is particularly important.

Here, we use a three-dimensional (3-D) chemical transport model (CTM) to investigate global CHBr_3 and CH_2Br_2 emission inventories. We perform the first concerted evaluation of three *top-down* and a single *bottom-up* derived inventory using

rate constants/absorption cross section data of Sander et al. (2011). For simulations here, the CTM used a prescribed monthly mean OH field which was used in TransCom-CH₄(?) and produced reasonable simulations of methyl chloroform (CH₃CCl₃) and CH₄.

2.1 Biogenic emissions from the ocean

Given the significant uncertainty in global VSLs emissions, TOMCAT was run for the period 1 January 1997 to 31 December 2011 with 4 previously published oceanic CHBr₃ and CH₂Br₂ emission inventories. Run S_{Liang} used the *top-down* emission fluxes of Liang et al. (2010) (hereafter “Liang-2010”). Run S_{Warwick} used the *top-down* estimates described in Warwick et al. (2006) and updated in Pyle et al. (2011) (hereafter “Warwick-2011”). Run S_{Ordóñez} used the top-down estimates of Ordóñez et al. (2012) (“Ordóñez-2012”). Finally, run S_{Ziska} used the *bottom-up* emission fluxes proposed by Ziska et al. (2013) (“Ziska-2013”). The global total emissions for each source gas under each scenario is given in Table 1.

The Warwick-2011 scenario is a top-down estimate based on the original work of Warwick et al. (2006). Aircraft observations of CHBr₃ and CH₂Br₂, collected during the 1999 National Aeronautics and Space Administration (NASA) Pacific Exploratory Mission (PEM) Tropics B, were used to constrain surface emissions. The updated scenario used here is based on scenario 5 outlined in Warwick et al. (2006), however South-east Asian CHBr₃ emissions have been scaled down to give agreement with surface observations collected at Danum Valley, Borneo. This updated scenario is further described in Pyle et al. (2011).

The Liang-2010 scenario is also a model top-down estimate constrained by aircraft observations. These observations were mostly concentrated around the Pacific and North America between 1996–2008 and include the following campaigns: PEM-Tropics, TRACE-P, INTEX, TC4, ARCTAS, STRAT, Pre-AVE and AVE (Liang et al., 2010). The emissions were formulated using a baseline scenario from Warwick et al. (2006), which was adjusted in both magnitude/location, so that modelled CHBr₃ and

Evaluating emissions of biogenic bromocarbons

R. Hossaini et al.

Title Page

Abstract

Introduction

Conclusions

References

Tables

Figures

⏪

⏩

◀

▶

Back

Close

Full Screen / Esc

Printer-friendly Version

Interactive Discussion



CH₂Br₂ gave good agreement with observations in the mid-troposphere, and the observed vertical gradient was well represented. The spatial distribution of emissions is assumed to be equal for CHBr₃ and CH₂Br₂.

The Ordóñez2012 scenario is the third top-down estimate. It is formulated using the same aircraft observations as Liang-2010 but also includes those obtained during the NASA POLARIS and SOLVE missions. This scenario is relatively sophisticated as, in the tropics ($\pm 20^\circ$), VLSL emissions are weighted towards the concentration of chlorophyll *a* (chl *a*); a potential proxy for oceanic bio-productivity. A monthly-varying satellite chl *a* climatology was used which allows some seasonality in the magnitude of the CHBr₃ and CH₂Br₂ emission fields. This is the only inventory to consider such seasonality. Outside of tropical latitudes the sea-air flux is constant with coastal emissions assumed to be a factor of 2.5 larger than the open ocean

Finally, the Ziska-2013 scenario is a bottom-up estimate of emissions. Based on data of the HalOcAt database project (<https://halocat.geomar.de/>), global surface marine and atmospheric concentration maps of CHBr₃, CH₂Br₂ (and CH₃I) were calculated in order to derive global sea-to-air flux estimates. The available in-situ measurements were classified according to current knowledge about the distribution and possible sources of each compound, as well as the physical and biogeochemical characteristics of ocean and atmosphere. Missing $1^\circ \times 1^\circ$ grid values were extrapolated with the Ordinary Least Square (OLS) regression technique depending on longitude and latitude. The OLS method includes outliers and thus represents the spread and variable concentration distribution well. Based on the generated marine and atmospheric surface concentration maps, global climatological emission maps were calculated with a commonly used sea-to-air flux parameterisation. This applied highly temporal (6 hourly) resolved wind speed, sea surface temperature, salinity and pressure data (Ziska et al., 2013).

Global emission maps for CHBr₃ and CH₂Br₂ are shown in Figs. 1 and 2, respectively. All scenarios differ significantly over the tropical West Pacific – an important region for the troposphere-stratosphere transport of VLSL (e.g., Aschmann et al., 2009)

Evaluating
emissions of
biogenic
bromocarbons

R. Hossaini et al.

Title Page

Abstract

Introduction

Conclusions

References

Tables

Figures

⏪

⏩

◀

▶

Back

Close

Full Screen / Esc

Printer-friendly Version

Interactive Discussion



and where observations of these species are limited. The latitudinal-dependence of emissions is shown in Fig. 3. For CHBr_3 , significant variation between the top-down derived estimates (Warwick-2011, Liang-2010, Ordóñez-2012) and the bottom-up estimate (Ziska-2013) is apparent – particularly in the tropics ($\pm 20^\circ$) and at high latitudes ($> 60^\circ$) in the Northern Hemisphere (NH). For CH_2Br_2 , the total global source strength between inventories is more consistent (Table 1), with the exception of Warwick-2011 in which it is $\sim 1.7\times$ larger than the others. Both Warwick-2011 and Ziska-2013 exhibit a significantly stronger CH_2Br_2 emission in the tropics relative to Liang-2010 and Ordóñez-2012. The Ziska-2013 inventory also contains particularly strong emissions in the Southern Hemisphere (see Ziska et al., 2013).

For minor VSLS (CHBr_2Cl , CHBrCl_2 and CH_2BrCl), emissions are not specified, rather their surface abundance is constrained using an assumed uniform volume mixing ratio (0.3, 0.3, 0.5 ppt) based on compiled observations in the tropical MBL (Montzka et al., 2011). Note, Warwick et al. (2006) and Ordóñez et al. (2012) reported emissions for these species but they are not available at present from the other inventories considered. While these minor VSLS are not the focus of this work, they are included in the calculation of $\text{Br}_y^{\text{VSLS}}$ in Sect. 6. As their nominal lifetime is relatively long-lived at the surface (59, 78 and 137 days) (Montzka et al., 2011), the spatial distribution of emission is less important for their troposphere-stratosphere transport (relative to CHBr_3).

3 Evaluation of emission inventories with long-term ground-based observations

Previous model studies have used aircraft observations to validate simulated VSLS profiles in the upper troposphere (e.g., Liang et al., 2010; Ashfold et al., 2012; Hossaini et al., 2012b; Ordóñez et al., 2012). Ideally, global models should be evaluated against observations from multiple platforms. For VSLS, whose emissions are poorly constrained and represent a significant uncertainty in global-scale models, a robust validation of available emissions inventories with ground-based observations is desirable.

Evaluating emissions of biogenic bromocarbons

R. Hossaini et al.

Title Page

Abstract

Introduction

Conclusions

References

Tables

Figures



Back

Close

Full Screen / Esc

Printer-friendly Version

Interactive Discussion



As the troposphere-stratosphere transport of VSLs is highly dependant on the location of emission (Aschmann et al., 2009), validation of both the spatial distribution and magnitude of emissions is needed. However, to date an evaluation of published emission inventories has yet to be performed.

In this study, multi-annual observations of CHBr_3 and CH_2Br_2 at 14 ground-based stations (Table 2) have been used to validate modelled fields and test emission estimates. The observed data are from an ongoing cooperative flask sampling program of the National Oceanic and Atmospheric Administration/Earth System Research Laboratory (NOAA/ESRL). Figure 4 shows the location of observations. Whole air samples (WAS) were collected approximately weekly into paired steel or glass flasks and were analysed using gas chromatography/mass spectrometry (GC-MS) (Montzka et al., 2003). NOAA data from flasks collected at surface sites and also on the HIPPO aircraft campaign are presented relative to the NOAA-2003 scale for CH_2Br_2 and the NOAA-2004 scale for CHBr_3 . These scales consist of 2–4 standards prepared with gravimetric techniques at 3–20 ppt in high-pressure (900 psi initially) 30 L, electropolished stainless steel canisters.

Figure 5 shows the NOAA/ESRL observed CHBr_3 mixing ratio at these stations (north-south). The observed data points are monthly mean fields that have been calculated from a 14 yr monthly mean data set (i.e. we have taken the mean of monthly mean fields). This approach smooths intra-monthly variability but can give a clear signal of seasonal variations. The observations spanned the period 1 January 1998 to 1 January 2012 at all stations except SPO, THD, and SUM, which are shorter records. Also shown on Fig. 5 is the corresponding modelled CHBr_3 mixing ratio from runs S_{Liang} , S_{Warwick} , S_{Ordonez} and S_{Ziska} . The CTM was run for the same (14 yr) period following 3 yr of spin up. Monthly mean data was output allowing a like-for-like comparison between model and observation.

At NH high latitude ($\geq 60^\circ$) stations (ALT, SUM and BRW), observed CHBr_3 exhibits a pronounced seasonal cycle with elevated mixing ratios during NH winter (DJF). This seasonality, likely due to the enhanced photochemical sink of CHBr_3 during summer

Evaluating emissions of biogenic bromocarbons

R. Hossaini et al.

Title Page

Abstract

Introduction

Conclusions

References

Tables

Figures

⏪

⏩

◀

▶

Back

Close

Full Screen / Esc

Printer-friendly Version

Interactive Discussion

Evaluating emissions of biogenic bromocarbons

R. Hossaini et al.

Title Page

Abstract

Introduction

Conclusions

References

Tables

Figures

⏪

⏩

◀

▶

Back

Close

Full Screen / Esc

Printer-friendly Version

Interactive Discussion

(JJA) months (or potentially transport), has been previously observed (at ALT) by Yokouchi et al. (1996). The CTM captures this seasonality, particularly at ALT and SUM, where the bias between model and observation is highly dependent on the emission inventory used. The top-down inventories (Liang-2010, Warwick2011 and Ordóñez-2012) on average underestimate observed CHBr_3 at these high latitude NH stations (Fig. 5). The calculated mean bias (model minus observation) for the entire 14 yr monthly-mean data set is -0.65 , -1.61 and -0.88 ppt for these inventories, respectively. The bottom-up estimate of Ziska-2013 overestimates with a positive mean bias of $+0.54$ ppt. This is skewed by the significant overestimation of CHBr_3 at ALT. It was previously shown in Fig. 3 that Ziska-2013 exhibits a significantly larger CHBr_3 source at high NH latitudes over the other inventories considered.

At NH mid-latitude (30 – 60° N) stations (MHD, LEF, HFM, THD and NWR), the agreement between model and observation varies significantly with emission inventory. At Mace Head (MHD), the top-down inventories underestimate the large background CHBr_3 (up to ~ 8 ppt). However, the larger bottom-up emissions of Ziska-2013 in this region lead to a reasonable agreement between model and observation. Note, here the seasonal cycle is out of expected phase, as a CHBr_3 minimum is observed during winter months and a maximum during summer. Carpenter et al. (2005) observed a similar seasonality and deduced that strong local emissions (during summer) dominate over enhanced photochemical loss to control the local CHBr_3 abundance at MHD.

For VSLS, transport to the stratosphere is most efficient in tropical regions where convection can rapidly loft boundary layer air into the mid/upper troposphere (e.g., Aschmann et al., 2009). At tropical ($\pm 30^\circ$) stations KUM and MLO there is also noticeable seasonality in observed CHBr_3 . This is in phase with most other NH stations and indicative of larger-scale processes (likely the photochemical sink) controlling the seasonality. The bias between the model and observation is again varied and strongly dependent on emission inventory. The Ordóñez-2012 emissions, which are weighted towards a seasonal climatology of chlorophyll *a* in the tropics, lead to an overestimate of CHBr_3 at each tropical station (KUM, MLO and SMO), and for all months. For these stations

the mean bias is 0.12, 0.48, 0.76 and 0.07 ppt for runs S_{Liang} , S_{Warwick} , $S_{\text{Ordóñez}}$ and S_{Ziska} , respectively. This indicates that the Liang-2010 (top-down) and the Ziska-2013 (bottom-up) derived CHBr_3 emissions perform particularly well at these locations in the tropical Pacific.

In the SH, long-term observations of VSLs are particularly sparse. In the SH mid-latitude ($30\text{--}60^\circ\text{S}$) band, data from just one station is available (CGO). Here, CHBr_3 is generally underestimated but reasonable agreement is obtained with the Liang-2010 and Ordóñez-2012 inventories. This is also the case at the two high-latitude SH stations ($60\text{--}90^\circ\text{S}$) PSA and SPO. Here, a clear seasonal cycle is apparent at the latter with a CHBr_3 maximum occurring during SH winter (JJA) – consistent with Swanson et al. (2004) and Beyersdorf et al. (2010) who note a similar seasonality. The CTM is able to reproduce this seasonality well and again the Liang-2010 and Ordóñez-2012 scenarios provide the best agreement.

For CH_2Br_2 , a similar comparison between the observations and the model has been performed (Fig. 6). Photolysis is a minor tropospheric sink for CH_2Br_2 , which has a nominal surface lifetime of ~ 120 days (Montzka et al., 2011), and whose dominant sink is by reaction with OH. As its lifetime is significantly longer than that of CHBr_3 (~ 26 days), horizontal gradients are expected to be less pronounced. The observations show background mixing ratios in the range of $\sim 0.5\text{--}1.5$ ppt at all stations (excluding MHD) with generally low variability. Seasonality is apparent at most sites in the NH (e.g. ALT, SUM, LEF, NWR, KUM, MLO etc.), and is likely due to seasonal changes to the $\text{CH}_2\text{Br}_2 + \text{OH}$ loss rate. The magnitude of relative variation is smaller than that for CHBr_3 due to the significantly longer lifetime of CH_2Br_2 .

The global CH_2Br_2 source strength is relatively similar for 3 out of the 4 inventories considered; $62\text{--}67\text{Ggyr}^{-1}$, among Liang-2010, Ordóñez-2012 and Ziska-2013. However, it is significantly larger (113Ggyr^{-1}) in the Warwick-2011 inventory. Also, the latitudinal distribution of emissions, including in the tropics, varies significantly between inventories (e.g. Fig. 3). At tropical stations KUM, MLO and SMO, CH_2Br_2 is overestimated when using Warwick-2011 and Ziska-2013 emissions. At these sta-

Evaluating emissions of biogenic bromocarbons

R. Hossaini et al.

Title Page

Abstract

Introduction

Conclusions

References

Tables

Figures

⏪

⏩

◀

▶

Back

Close

Full Screen / Esc

Printer-friendly Version

Interactive Discussion

Evaluating emissions of biogenic bromocarbons

R. Hossaini et al.

Title Page

Abstract

Introduction

Conclusions

References

Tables

Figures

⏪

⏩

◀

▶

Back

Close

Full Screen / Esc

Printer-friendly Version

Interactive Discussion



tions, improved agreement is obtained using Ordóñez-2012 and good agreement using Liang-2010. In the SH, between $\sim 40\text{--}75^\circ\text{S}$, the Ziska-2013 inventory exhibits a particularly strong CH_2Br_2 source (see Fig. 3), not featured in the other inventories. Comparison of modelled CH_2Br_2 with observations within this latitude range (i.e. CGO and PSA sites), show a significant overestimation of CH_2Br_2 , by an approximate factor of 2, when using the Ziska-2013 inventory.

For a more quantitative evaluation of the modelled CHBr_3 and CH_2Br_2 fields with these long-term surface observations, three error metrics were calculated (Tables 3 and 4); the mean bias (MB) (ppt), calculated using (Eq. 1), the mean absolute deviation (MAD) (ppt), calculated using (Eq. 2), and the mean absolute percentage error (MAPE), using (Eq. 3), for the 5 latitudinal bands considered. Here, M and O denote the monthly modelled and observed fields for the entire 14 yr period of comparison, respectively. The total number of comparison points (n) is 168.

$$\text{MB} = \frac{1}{n} \sum_{t=1}^n (M_t - O_t) \quad (1)$$

$$\text{MAD} = \frac{1}{n} \sum_{t=1}^n |M_t - O_t| \quad (2)$$

$$\text{MAPE} = \frac{100}{n} \sum_{t=1}^n \left| \frac{M_t - O_t}{O_t} \right| \quad (3)$$

Based on the reported error metrics it is clear the performance of each inventory varies significantly by region. Focusing on the important tropical latitude band, for CHBr_3 the MAPE between model and observation ranges between 36 % to 115 %. The best agreement, diagnosed by the lowest MAPE (36 %), is obtained from run S_{Ziska} (bottom-up emissions). S_{Liang} also performs well in the tropics with a similar MAPE of 38 %, which is significantly lower than runs S_{Warwick} and S_{Ordonez} . Note, small values of observed CHBr_3 can cause large skew in the calculated MAPE (see Eq. 3). For CH_2Br_2 ,

MAPE ranges from 24–166% in the tropics. The best agreement is obtained from run S_{Liang} (24%), using the Liang-2010 inventory which has the lowest total emissions in the tropics and also the lowest global total (see Fig. 3 also). The calculated mean bias presented in Table 4 confirms the significant overestimation of CH_2Br_2 by runs S_{Warwick} and S_{Ziska} suggesting a significant overestimate of the tropical CH_2Br_2 source in these emissions inventories.

Overall, the global performance (all stations) of each scenario can be assessed based on the error metrics in Table 3. Globally, the best agreement between model and observation, for both CHBr_3 and CH_2Br_2 , is obtained for run S_{Liang} . The global MAPE using the Liang-2010 inventory is 50% and 20% for these species, respectively. To support this conclusion, further long-term observations of VSLS would be desirable, particularly in the tropics and in the poorly sampled Southern Hemisphere. While the NOAA/ESRL observations are a valuable long-term record, the spatial distribution of sampling is limited in these regions. Therefore, we also consider recent aircraft observations of CHBr_3 and CH_2Br_2 made during the HIPPO aircraft campaigns over the Pacific basin that spanned global latitudes (Sect. 4). Observations of VSLS made in the poorly sampled tropical West Pacific during the SHIVA campaign are also considered in a case study (Sect. 5).

The error metrics presented in Tables 3 and 4 were computed for all months. To examine any potential systematic seasonal bias between the model and the observations, probability density functions (PDF) have been computed by season and latitude band (see Supplement). For both CHBr_3 and CH_2Br_2 , no clear systematic seasonal bias is apparent. The skill of the model in reproducing the observations is highly dependent on the magnitude/distribution of emissions, which were previously shown to vary significantly. The seasonality of these gases, observed at numerous ground-based stations, is generally well captured by aseasonal emissions (3 of the 4 inventories). This suggests at these sites, the seasonality is largely driven by photochemistry (i.e. sinks) that are well represented in the model.

Evaluating emissions of biogenic bromocarbons

R. Hossaini et al.

[Title Page](#)[Abstract](#)[Introduction](#)[Conclusions](#)[References](#)[Tables](#)[Figures](#)[Back](#)[Close](#)[Full Screen / Esc](#)[Printer-friendly Version](#)[Interactive Discussion](#)

4 Evaluation of emission inventories with HIPPO aircraft data

The HIAPER Pole-to-Pole Observations (HIPPO) project consisted of a series of aircraft campaigns between 2009–2011 supported by the National Science Foundation (NSF). Five missions were conducted (January 2009, November 2009, March/April 2010, June 2011 and August/September 2011). The aim of HIPPO was to make global measurements of various trace gases, including greenhouse gases CO₂, CH₄, N₂O and also CO, SF₆, CFCs and bromine-containing VSLs (Wofsy et al., 2011). Sampling spanned a range of latitudes, from near the North Pole to coastal Antarctica, on board the NSF Gulfstream V aircraft and from the surface to ~ 14 km over the Pacific basin. As such, these comprehensive data complement the long-term observations of VSLs discussed in Sect. 3 and allow for further evaluation of the model with varying emissions inventories of CHBr₃ and CH₂Br₂. The HIPPO data is particularly valuable for this analysis as it is independent, i.e. has not been used in constructing the emission inventories considered. The data is archived at the following web address: <http://www.eol.ucar.edu/projects/hippo/>.

Figures 7 and 8 compare mean observed profiles of CHBr₃ and CH₂Br₂, made during HIPPO 1–5, with modelled TOMCAT profiles for the 5 latitude bands considered in this work. The observations here were collected using whole air samples, in stainless steel and glass flasks, and analysed by two different laboratories by gas chromatography/mass spectrometry (GC-MS); NOAA/ESRL and the University of Miami. Mixing ratios from HIPPO are reported on the same calibration scale as the NOAA/ESRL ground-based station results. The model has here been sampled for each flighttrack to match the observations and allowing a point-by-point comparison throughout the profiles. To assess the skill of the model against the HIPPO observations, three error metrics were again computed; the mean bias (MB) (ppt), calculated using (Eq. 1), the mean absolute deviation (MAD) (ppt), calculated using (Eq. 2), and the mean absolute percentage error (MAPE), using (Eq. 3), for the 5 latitudinal bands considered. These are summarised in Tables 5 and 6 for CHBr₃ and CH₂Br₂, respectively.

Evaluating emissions of biogenic bromocarbons

R. Hossaini et al.

Title Page

Abstract

Introduction

Conclusions

References

Tables

Figures

⏪

⏩

◀

▶

Back

Close

Full Screen / Esc

Printer-friendly Version

Interactive Discussion



Evaluating emissions of biogenic bromocarbons

R. Hossaini et al.

Title Page

Abstract

Introduction

Conclusions

References

Tables

Figures

⏪

⏩

◀

▶

Back

Close

Full Screen / Esc

Printer-friendly Version

Interactive Discussion



observation is obtained from runs S_{Liang} and S_{Ziska} , where MAPE is $\sim 40\%$ for both. This supports the findings of Sect. 3, where it was also shown that the Liang-2010 and Ziska-2013 emission inventories give the best agreement with long-term NOAA/ESRL ground-based observations of CHBr_3 . Note, while the global MAPE happens to be similar for these two runs, differences within the 5 latitudes bands are apparent. For example, in the tropics ($\pm 30^\circ$), as noted, the better agreement is obtained from the lower (Ziska-2013) bottom-up emissions (MAPE $\sim 35\%$). In fact, this is the only inventory that results in a MAPE $< 50\%$ for CHBr_3 in the tropics, suggesting overestimated emissions in this region from the top-down inventories.

The model is also able to reproduce the observed distribution of CH_2Br_2 well. Again, the overall skill of the model is highly dependent on the given emission inventory. For each of the 5 latitude bands considered, the best agreement between the model and observation is obtained from run S_{Liang} . The calculated MAPE for this run is $< 25\%$ within each latitude band and globally is $\sim 18\%$. This supports the findings of the ground-based analysis presented in Sect. 3, where the Liang-2010 emission inventory, which has the lowest total emissions of $62 \text{ Gg CH}_2\text{Br}_2 \text{ yr}^{-1}$ (Table 1), was shown to perform particularly well. Note, the Ordóñez-2012 inventory also performs well for CH_2Br_2 with a global MAPE of $\sim 24\%$. This is a significantly better agreement than that obtained from the Warwick-2011 (87%) and Ziska-2013 inventories (63%) that generally lead to overestimation of CH_2Br_2 . Overall, for both CHBr_3 and CH_2Br_2 the calculated biases between the model and the HIPPO aircraft data are consistent with, and support the findings of, the comparisons with the NOAA/ESRL ground-based observations.

5 A case study in the tropical West Pacific

The tropical West Pacific is a region of frequent and intense convection resulting in efficient transport of boundary layer air into the tropical tropopause layer (TTL) (e.g., Fueglistaler et al., 2009; Krüger et al., 2009). A number of model studies have reported

Evaluating emissions of biogenic bromocarbons

R. Hossaini et al.

Title Page

Abstract

Introduction

Conclusions

References

Tables

Figures

⏪

⏩

◀

▶

Back

Close

Full Screen / Esc

Printer-friendly Version

Interactive Discussion

the importance of the tropical West Pacific for the transport of VSLs into the stratosphere (e.g., Levine et al., 2007; Aschmann et al., 2009). The region is poorly sampled and local emissions, including those from farmed seaweed species (Leedham et al., 2013), are uncertain. Previous regional observations of VSLs include those made during the OP3 campaign on Borneo (Pyle et al., 2011). Background CHBr_3 was reported at ~ 1 ppt inland (Danum Valley) with a larger background (2–5 ppt) reported along the coast (Kunak).

Figure 9 shows the modelled 2011 mean surface mixing ratio of CHBr_3 over the tropical West Pacific. Different emission inventories lead to significant variation between the modelled CHBr_3 abundance. The largest modelled CHBr_3 in this region is from S_{Liang} and S_{Ordonez} with ~ 3.25 and 3.0 ppt around the northern coast of Borneo. These emission inventories were derived with little or no observations in the tropical Western Pacific (see Liang et al., 2010 and Ordóñez et al., 2012). Runs S_{Warwick} and S_{Ziska} show significantly lower CHBr_3 (~ 2 ppt) and this is likely due to the use of regional observations in the formulation of these inventories. Warwick-2011 was derived with regional scaling to give good agreement with observations made during OP3 on Borneo, while Ziska-2013, the bottom-up estimate, included CHBr_3 sea-air flux data measured in this region during the Trans-Brom cruise (Krüger and Quack, 2012). For surface CH_2Br_2 (also Fig. 9), the modelled mixing ratio is typically between ~ 1.0 to 1.5 ppt in the region of Borneo for all runs. The exception is run S_{Warwick} , where it is ~ 1 ppt greater (i.e. ~ 2.0 – 2.5 ppt) due to the larger regional emissions in the Warwick-2011 inventory. The remainder of Sect. 5 evaluates the CTM and emission inventories in this region using recent aircraft observations made in the free troposphere during the 2011 SHIVA campaign.

5.1 The 2011 SHIVA campaign

The Stratospheric Ozone: Halogen Impacts in a Varying Atmosphere (SHIVA) campaign is a European Union (EU) funded research project (<http://shiva.iup.uni-heidelberg.de/>). A primary SHIVA objective is to investigate biogenic emissions of

VLSL, their atmospheric transformation, transport to the stratosphere and ultimately their impact on O₃. A field campaign was conducted during November–December 2011 in the tropical Western Pacific region based on Malaysian Borneo. An overview of the campaign is given in Pfeilsticker and the SHIVA consortium (2013).

5.1.1 Aircraft observations

Aircraft observations of VLSL in the tropical western Pacific region are extremely limited. Within the framework of SHIVA, aircraft observations of brominated VLSL were made during 14 flights on board the Deutsches Zentrum für Luft- und Raumfahrt (DLR) Falcon aircraft around Borneo. The flight tracks and location of sampling is shown in Fig. 10. Here we consider observations of major VLSL CHBr₃ and CH₂Br₂ made by the University of Frankfurt (UOF) and the University of East Anglia (UEA). These data are used to further evaluate the performance of the model, and top-down/bottom-up emission inventories, in the free troposphere within this poorly sampled region.

Observations made by the UOF group used the “Gaschromatograph for Observation of Stratospheric Tracers-Mass Spectrometer (GhOST-MS)” instrument – a fully automated GC/MS system for airborne (in-situ) observations of halogenated hydrocarbons. Observed mixing ratios for CHBr₃ and CH₂Br₂ from the GhOST-MS are reported on the NOAA-2003 calibration scale (see Sects. 3 and 4). The determined accuracy of the working standard gas is estimated at 16.5 % and 9.0 % for these species, respectively. The precision of the instrument varies between flights but is typically < 4 % for both species. For further details of the SHIVA aircraft observations see Sala et al. (2013).

Observations by UEA used the Falcon whole air sampler (WASP) that consisted of 30 glass flasks (approximately 700 mL internal volume) which were filled to a pressure of 2.5 Bar using a diaphragm pump. The samples were analysed for halocarbons within 48 hours of collection using a GC/MS (Agilent 6973) operating in negative ion, chemical ionisation mode (Worton et al., 2008). Because of a limitation of the sampling pump, WASP samples were only collected at altitudes below ~ 3 km. WASP data for CHBr₃ and CH₂Br₂ data are also reported on the most recent NOAA scales. Typical analytical

Evaluating emissions of biogenic bromocarbons

R. Hossaini et al.

Title Page

Abstract

Introduction

Conclusions

References

Tables

Figures

◀

▶

◀

▶

Back

Close

Full Screen / Esc

Printer-friendly Version

Interactive Discussion



precision (750 mL sample) was < 4 % for both compounds, with a calibration uncertainty of 7.1 % and 6.5 % for CHBr_3 and CH_2Br_2 , respectively. The two bromocarbon datasets will be examined in further detail in Sala et al. (2013).

Figure 11 shows the modelled mixing ratio of CHBr_3 sampled along the flight track of the Falcon aircraft during SHIVA. Also shown is the observed CHBr_3 mixing ratio from the GhOST-MS and WASP instruments. The observations show that during most flights, CHBr_3 rarely exceed 1.0–1.5 ppt. A notable exception is flight 4, during which CHBr_3 was elevated (> 2 ppt) near the surface. Large quantities of seaweed were visible from the aircraft during this flight, suggesting a large and localised emission source. Note, within the framework of SHIVA, emissions of halocarbons from both naturally-occurring, and farmed tropical macroalgae, has been investigated (Leedham et al., 2013).

The agreement between modelled and observed CHBr_3 is highly dependent on the emission inventory. As before, we have calculated the mean bias (MB) (ppt), the mean absolute deviation (MAD) (ppt) and the mean absolute percentage error (MAPE) (%) between the model and observation for all flights considered. For CHBr_3 , a summary of these metrics is given in Table 7. In general, the top-down inventories (Liang-2010, Warwick-2011, and Ordóñez-2012) overestimate the observations. This is particularly the case for runs S_{Liang} and $S_{\text{Ordóñez}}$ where CHBr_3 is overestimated, from the surface upto ~ 12 km, during numerous flights (e.g. flights 1a, 5b, 6 and 9a). The MB between model and observation for these flights is 1.75 ppt, 1.28 ppt, 1.31 ppt and 1.10 ppt for S_{Liang} and 1.69 ppt, 1.24 ppt, 1.26 ppt and 1.13 ppt for $S_{\text{Ordóñez}}$. Although also overestimating, an improved agreement is obtained from run S_{Warwick} in this region. For example, for the same flights the MB is smaller (i.e. $\text{MB} < 1$ ppt) at 0.88 ppt, 0.65 ppt, 0.79 ppt and 0.50 ppt. Overall, the best agreement is obtained from S_{Ziska} (bottom-up emissions), that for some flights exhibits a small negative bias. For the above flight, the MB is 0.38 ppt, 0.09 ppt, 0.15 ppt, and 0.30 ppt, respectively.

Across all the flights considered, the MAPE between the model and observed CHBr_3 is 146 %, 87 %, 156 % and 41 % for runs S_{Liang} , S_{Warwick} , $S_{\text{Ordóñez}}$ and S_{Ziska} ,

Evaluating emissions of biogenic bromocarbons

R. Hossaini et al.

Title Page

Abstract

Introduction

Conclusions

References

Tables

Figures

⏪

⏩

◀

▶

Back

Close

Full Screen / Esc

Printer-friendly Version

Interactive Discussion



Evaluating emissions of biogenic bromocarbons

R. Hossaini et al.

Title Page

Abstract

Introduction

Conclusions

References

Tables

Figures

⏪

⏩

◀

▶

Back

Close

Full Screen / Esc

Printer-friendly Version

Interactive Discussion

respectively – highlighting the significant variation in the performance of the inventories in this region. The bottom-up CHBr_3 emissions proposed by Ziska et al. (2013) perform particularly well as this is the only inventory that gives rise to a MAPE < 50 % in this region. This inventory was also shown to perform well against the NOAA/ESRL ground-based observations (Sect. 3) and HIPPO aircraft observations (Sect. 4) in the tropical Pacific basin. The Ziska-2013 inventory is constrained by local sea-to-air fluxes obtained in the tropical West Pacific during ship cruises; e.g., Trans-Brom (Krüger and Quack, 2012). This is the likely explanation as to why the MAPE is significantly lower for this inventory, over Liang-2010 and Ordóñez-2012, that are based on limited or no regional (aircraft) observations. The same is true of the Warwick-2011 inventory, which also performs relatively well in this region, and is constrained by local (ground-based) observations. This further highlights the need for more local observations of VSLs, particularly in poorly sampled regions, in order to improve VSLs emission inventories at the regional scale.

Figure 12 shows the modelled versus observed CH_2Br_2 during SHIVA flights. The observations show CH_2Br_2 typically in the range of 0.5–1.5 ppt during most flights and with a relatively small vertical gradient. The performance of each emission inventory is assessed using the error metrics summarised in Table 8. Across all flights, the MAPE is generally low at 26 %, 121 %, 36 % and 57 % for runs S_{Liang} , S_{Warwick} , $S_{\text{Ordóñez}}$ and S_{Ziska} , respectively. Consistent with the NOAA/ESRL ground-based analysis (Sect. 3) and also the HIPPO aircraft analysis (Sect. 4), the best agreement (diagnosed by lowest MAPE) between modelled and observed CH_2Br_2 , is obtained by S_{Liang} . For run S_{Warwick} , that was previously shown to overestimate surface CH_2Br_2 at NOAA/ESRL stations in the Pacific basin (e.g. Fig. 6), we again find an overestimate against SHIVA observations (approximate factor of 2). Therefore, it seems highly likely that the CH_2Br_2 emission strength is significantly overestimated in the tropics by the Warwick-2011 inventory.

6 Sensitivity of stratospheric bromine loading to emission inventory

In our previous modelling work, emissions of major VLSLs CHBr_3 and CH_2Br_2 were not specified in the TOMCAT CTM (Hossaini et al., 2010, 2012b). Rather, a uniform surface mixing ratio (~ 1.2 ppt) was imposed in the tropics ($\pm 20^\circ$) based on compiled aircraft observations. Using this approach, Hossaini et al. (2012b) quantified stratospheric $\text{Br}_y^{\text{VLSL}}$ as ~ 5 ppt; i.e., within the compiled range of 1–8 ppt outlined in WMO (2011), and in general agreement with balloon-borne estimates (Dorf et al., 2006, 2008). The CTM performed reasonably well against aircraft observations in the TTL. However, this approach meant regional *hot-spots*, where emissions may be large and background concentrations elevated, were not captured. Any dependence of stratospheric $\text{Br}_y^{\text{VLSL}}$ on the spatial distribution of surface emissions was also not modelled. Here, using the CTM runs presented in this paper (i.e. multiple emission inventories for CHBr_3 and CH_2Br_2), we revise our estimate of $\text{Br}_y^{\text{VLSL}}$ based on these spatially varying, and seasonally-varying in the case of Ordóñez-2012, emission inventories.

It is thought that VLSLs contribute to the stratospheric bromine budget via both source gas injection (SGI) and also product gas injection (PGI). The SGI pathway is quantified by summing the total organic bromine from VLSLs reaching the lower stratosphere. For PGI, which refers to the troposphere-stratosphere transport of inorganic product gases (e.g. BrO , HBr), the tropospheric partitioning of Br_y among soluble and non-soluble species needs consideration. As this involves complex heterogeneous and multi-phase processes (e.g., Aschmann and Sinnhuber, 2013), which are crudely treated in global models, Br_y speciation and recycling represents a significant uncertainty in the quantification of PGI with models. The approach used here is identical to that described in Hossaini et al. (2012b). Once Br_y is released from source gases it is partitioned between soluble and non-soluble form according to a mean altitude-dependent $\text{HBr}:\text{Br}_y$ ratio. This was taken from a previous CTM integration in which detailed partitioning of tropospheric Br_y was considered.

Evaluating emissions of biogenic bromocarbons

R. Hossaini et al.

Title Page

Abstract

Introduction

Conclusions

References

Tables

Figures

⏪

⏩

◀

▶

Back

Close

Full Screen / Esc

Printer-friendly Version

Interactive Discussion

Figure 13 shows the modelled tropical mean profile of $\text{Br}_y^{\text{VLSL}}$ in the stratosphere at the end of the 14 yr simulation. We find $\text{Br}_y^{\text{VLSL}}$ ranges from $\sim 5\text{--}8$ ppt (above ~ 30 km) depending on the choice of emission inventory. Runs S_{Ziska} and S_{Warwick} account for the lower limit and upper limit, respectively. However, as S_{Warwick} overestimated both CHBr_3 and CH_2Br_2 significantly in the tropics, it seems likely that the upper limit of ~ 8 ppt reported here is also an overestimate. We have therefore now identified a range of uncertainty with regard to emissions of major VLSL CHBr_3 and CH_2Br_2 on stratospheric $\text{Br}_y^{\text{VLSL}}$ loading. Note, here $\text{Br}_y^{\text{VLSL}}$ includes the contribution from minor VLSL CHBr_2Cl , CHBrCl_2 and CH_2BrCl , which have not been the focus of this work, also. Their total contribution to $\text{Br}_y^{\text{VLSL}}$ is ~ 1 ppt and is consistent between each model run.

The modelled stratospheric $\text{Br}_y^{\text{VLSL}}$ ranges from $\sim 5\text{--}8$ ppt when both CHBr_3 and CH_2Br_2 are taken from the same inventory. However, in the tropics, where the troposphere-stratosphere transport of VLSL is most rapid, it was shown using ground-based (Sect. 3) and aircraft (Sect. 4) observations that a single inventory does not provide the simultaneous best agreement for both VLSL in this region. For CHBr_3 , the best agreement was obtained from run S_{Ziska} and similarly, for CH_2Br_2 , run S_{Liang} gave the best agreement. Therefore, we also report an *optimised* estimate of stratospheric $\text{Br}_y^{\text{VLSL}}$ based on a combination of these two fields; ~ 4 ppt (also shown on Fig. 13). From the 4 inventories considered, the CHBr_3 and CH_2Br_2 source strength is the lowest in Ziska-2013 and Liang-2010, respectively. Therefore, the optimised estimate reported here is lower than the range obtained when considering emissions of both species from the same inventory.

Our optimised $\text{Br}_y^{\text{VLSL}}$ estimate of ~ 4 ppt is lower than that reported in our previous work (~ 5 ppt) (Hossaini et al., 2012b), that did not use spatially-varying emission fluxes. The use of a fixed mixing ratio as a surface boundary condition for CHBr_3 and CH_2Br_2 in Hossaini et al. (2012b) may have overestimated their abundance in the boundary layer. However, our modelled optimised estimate is in good agreement with $\text{Br}_y^{\text{VLSL}}$ derived from observations of stratospheric BrO (the so-called *inorganic*

Evaluating emissions of biogenic bromocarbons

R. Hossaini et al.

Title Page

Abstract

Introduction

Conclusions

References

Tables

Figures

⏪

⏩

◀

▶

Back

Close

Full Screen / Esc

Printer-friendly Version

Interactive Discussion

method). For example, using Differential Optical Absorption Spectroscopy (DOAS) to obtain BrO profiles, combined with photochemical modelling, Dorf et al. (2006) reported a $\text{Br}_y^{\text{VLSL}}$ contribution of $4.1(\pm 2.5)$ ppt. However, given the recent findings of Kreycky et al. (2012) on the ratio of $J(\text{BrONO}_2)/k(\text{BrO}+\text{NO}_2)$, this estimate may need to be revised downward. Overall, our model calculations are consistent with the broad $\text{Br}_y^{\text{VLSL}}$ range of 1–8 ppt reported by WMO (2011).

7 Summary and Conclusions

Global models require a realistic treatment of biogenic bromine emissions in order to simulate a reasonable Br_y budget in both the troposphere and the stratosphere. At present, oceanic emissions of brominated VLSLs are poorly constrained and represent a significant uncertainty in global models (WMO, 2007, 2011). Given suggestions that stratospheric VLSL loading may increase in response to climate change (Dessens et al., 2009; Hossaini et al., 2012a), constraining both the magnitude and spatial distribution of contemporary emissions is important. In this study we have used a global model to perform the first concerted evaluation of previously published global CHBr_3 and CH_2Br_2 emission inventories. We have evaluated three top-down and a bottom-up derived inventory by comparing the simulated abundance of these VLSLs with independent observations – i.e. the observed data was not included in the formulation of the emission inventories. The observed data have included long-term observations at various NOAA/ESRL ground-based stations, aircraft observations made during the NSF HIPPO campaigns (1–5) and also novel aircraft observations made during the 2011 SHIVA campaign, over the poorly sampled tropical West Pacific. We have also updated our previous model estimate of $\text{Br}_y^{\text{VLSL}}$ based on these available emission scenarios.

Our comparisons reveal the TOMCAT CTM is able to reproduce a variety of global CHBr_3 and CH_2Br_2 observations. The agreement between the model and the observation is highly dependent on the choice of emission inventory, which differ significantly in terms of magnitude and spatial distribution. All the inventories considered give good

agreement in some locations. However, to accurately diagnose the source gas injection of VSLS into the stratosphere, simulating their abundance in the tropics, where transport to the stratosphere is rapid, is most important. Comparison of the model with observations at NOAA/ESRL surface sites and also with aircraft observations obtained during HIPPO, show a consistent pattern on the performance of individual emission inventories. Based on these comparisons, along with the results from the SHIVA case study, our main findings are:

- Current global emissions inventories of CHBr_3 and CH_2Br_2 , that are used in global models, vary significantly. Evaluating these inventories is challenging due to the limited spatial coverage of long-term observations, particularly in the tropics and in the Southern Hemisphere. Averaged globally, the best agreement between modelled CHBr_3 and CH_2Br_2 with long-term surface observations made by NOAA/ESRL is obtained using the top-down emissions proposed by Liang et al. (2010). Globally, the mean absolute percentage error between the model and NOAA/ESRL observations for this inventory is $\sim 50\%$ and $\sim 20\%$ for CHBr_3 and CH_2Br_2 over a 14 yr period, respectively. Comparison of the model with aircraft observations made during the HIPPO project, that spanned global latitudes over the Pacific basin, also support these findings. Globally, the mean absolute percentage error between the model and HIPPO observations is similar at 42% and 18% , for CHBr_3 and CH_2Br_2 respectively, when using the Liang et al. (2010) emissions. Globally, we also find the CH_2Br_2 emissions of Ordóñez et al. (2012) perform particularly well with a mean absolute percentage error of less than $\sim 30\%$ between model and observations.
- For CHBr_3 , within the tropics only, the best agreement between the model and observations is obtained using the bottom-up emission fluxes proposed by Ziska et al. (2013). Using this inventory, the mean absolute percentage error between the model and long term NOAA/ESRL surface observations is $\sim 36\%$. Against the HIPPO observations it is $\sim 35\%$, with the other inventories considered giving

Evaluating emissions of biogenic bromocarbons

R. Hossaini et al.

Title Page

Abstract

Introduction

Conclusions

References

Tables

Figures

⏪

⏩

◀

▶

Back

Close

Full Screen / Esc

Printer-friendly Version

Interactive Discussion



Evaluating emissions of biogenic bromocarbons

R. Hossaini et al.

Title Page

Abstract

Introduction

Conclusions

References

Tables

Figures

⏪

⏩

◀

▶

Back

Close

Full Screen / Esc

Printer-friendly Version

Interactive Discussion

tropics using three independent sets of observations (i.e. NOAA/ESRL surface, HIPPO aircraft and SHIVA aircraft data). Both the modelled range and optimised estimate are within the compiled 1–8 ppt range reported by WMO (2011). Therefore, in this study we have now identified the range of uncertainty associated with emissions of major VSLS CHBr_3 and CH_2Br_2 on stratospheric $\text{Br}_y^{\text{VSLS}}$ loading. Although, model estimates of the product gas injection contribution to $\text{Br}_y^{\text{VSLS}}$ remain a significant uncertainty (e.g, Salawitch et al., 2010; Aschmann and Sinnhuber, 2013).

Our study has shown that in recent years understanding of oceanic VSLS emissions has improved significantly and that current inventories used in global models are reasonable. Based on the results of this work, it would be useful to revise current inventories and/or combine them to improve the treatment of CHBr_3 and CH_2Br_2 emissions in global models. Furthermore, it would be useful for the analysis performed in this study to be repeated by other modelling groups, in order to determine the extent to which our results are model-dependent. For example, to assess the role of differences in model transport, such as mixing in the boundary layer and convection, which are parameterized and likely to vary between models. A related exercise examining inter-model variability on the tropospheric distribution and the troposphere-stratosphere transport of VSLS is planned, within the framework of the ongoing Atmospheric Tracer Transport Model Intercomparison (TRANSCOM) project (e.g., Patra et al., 2011). Finally, future work will examine emissions of relatively minor VSLS (e.g. CHBr_2Cl , CH_2BrCl) along with a more detailed examination of emission seasonality.

Supplementary material related to this article is available online at:
<http://www.atmos-chem-phys-discuss.net/13/12485/2013/acpd-13-12485-2013-supplement.pdf>.

Acknowledgements. This work was supported by the UK Natural Environment Research Council (NERC) and the EU Stratospheric Ozone: Halogen Impacts in a Varying Atmosphere (SHIVA) project (SHIVA-226224-FP7-ENV-2008–1). TOMCAT work is supported by the National Centre for Atmospheric Science (NCAS). NOAA measurements were supported in part by NOAA's Atmospheric Chemistry, Carbon Cycle and Climate Program of its Climate Program Office. Technical assistance, standardization, and programmatic support for NOAA flask measurements was provided by C. Siso, B. Hall, and J.W. Elkins. The HIPPO project was supported by the National Science Foundation (NSF).

References

- Aschmann, J. and Sinnhuber, B.-M.: Contribution of very short-lived substances to stratospheric bromine loading: uncertainties and constraints, *Atmos. Chem. Phys.*, 13, 1203–1219, doi:10.5194/acp-13-1203-2013, 2013. 12489, 12506, 12511
- Aschmann, J., Sinnhuber, B.-M., Atlas, E. L., and Schauffler, S. M.: Modeling the transport of very short-lived substances into the tropical upper troposphere and lower stratosphere, *Atmos. Chem. Phys.*, 9, 9237–9247, doi:10.5194/acp-9-9237-2009, 2009. 12492, 12494, 12495, 12502
- Ashfold, M. J., Harris, N. R. P., Atlas, E. L., Manning, A. J., and Pyle, J. A.: Transport of short-lived species into the Tropical Tropopause Layer, *Atmos. Chem. Phys.*, 12, 6309–6322, doi:10.5194/acp-12-6309-2012, 2012. 12493
- Beyersdorf, A. J., Blake, D. R., Swanson, A., Meinardi, S., Rowland, F. S., and Davis, D.: Abundances and variability of tropospheric volatile organic compounds at the South Pole and other Antarctic locations, *Atmos. Environ.*, 44, 4565–4574, doi:10.1016/j.atmosenv.2010.08.025, 2010. 12496
- Breider, T. J., Chipperfield, M. P., Richards, N. A. D., Carslaw, K. S., Mann, G. W., and Spracklen, D. V.: Impact of BrO on dimethylsulfide in the remote marine boundary layer, *Geophys. Res. Lett.*, 37, L02807, doi:10.1029/2009gl040868, 2010. 12488
- Brinckmann, S., Engel, A., Bönisch, H., Quack, B., and Atlas, E.: Short-lived brominated hydrocarbons – observations in the source regions and the tropical tropopause layer, *Atmos. Chem. Phys.*, 12, 1213–1228, doi:10.5194/acp-12-1213-2012, 2012. 12489

Evaluating emissions of biogenic bromocarbons

R. Hossaini et al.

Title Page

Abstract

Introduction

Conclusions

References

Tables

Figures



Back

Close

Full Screen / Esc

Printer-friendly Version

Interactive Discussion



**Evaluating
emissions of
biogenic
bromocarbons**

R. Hossaini et al.

Title Page

Abstract

Introduction

Conclusions

References

Tables

Figures

⏪

⏩

◀

▶

Back

Close

Full Screen / Esc

Printer-friendly Version

Interactive Discussion

- Carpenter, L. and Liss, P.: On temperate sources of bromoform and other reactive organic bromine gases, *J. Geophys. Res.-Atmos.*, 105, 20539–20547, doi:10.1029/2000jd900242, 2000. 12488
- Carpenter, L. J., Wevill, D. J., O'Doherty, S., Spain, G., and Simmonds, P. G.: Atmospheric bromoform at Mace Head, Ireland: seasonality and evidence for a peatland source, *Atmos. Chem. Phys.*, 5, 2927–2934, doi:10.5194/acp-5-2927-2005, 2005. 12489, 12495
- Chipperfield, M. P.: New Version of the tomcat/slimcat off-line chemical transport model: inter-comparison of stratospheric tracer experiments, *Q. J. Roy. Meteor. Soc.*, 132, 1179–1203, doi:10.1256/Qj.05.51, 2006. 12490
- Dessens, O., Zeng, G., Warwick, N., and Pyle, J.: Short-lived bromine compounds in the lower stratosphere; impact of climate change on ozone, *Atmos. Sci. Lett.*, 10, 201–206, doi:10.1002/asl.236, 2009. 12489, 12508
- Dorf, M., Butler, J. H., Butz, A., Camy-Peyret, C., Chipperfield, M. P., Kritten, L., Montzka, S. A., Simmes, B., Weidner, F., and Pfeilsticker, K.: Long-term observations of stratospheric bromine reveal slow down in growth, *Geophys. Res. Lett.*, 33, L24803, doi:10.1029/2006gl027714, 2006. 12489, 12506, 12508
- Dorf, M., Butz, A., Camy-Peyret, C., Chipperfield, M. P., Kritten, L., and Pfeilsticker, K.: Bromine in the tropical troposphere and stratosphere as derived from balloon-borne BrO observations, *Atmos. Chem. Phys.*, 8, 7265–7271, doi:10.5194/acp-8-7265-2008, 2008. 12489, 12506
- Feng, W., Chipperfield, M. P., Dorf, M., Pfeilsticker, K., and Ricaud, P.: Mid-latitude ozone changes: studies with a 3-D CTM forced by ERA-40 analyses, *Atmos. Chem. Phys.*, 7, 2357–2369, doi:10.5194/acp-7-2357-2007, 2007. 12488
- Feng, W., Chipperfield, M. P., Dhomse, S., Monge-Sanz, B. M., Yang, X., Zhang, K., and Ramonet, M.: Evaluation of cloud convection and tracer transport in a three-dimensional chemical transport model, *Atmos. Chem. Phys.*, 11, 5783–5803, doi:10.5194/acp-11-5783-2011, 2011. 12490
- Fueglistaler, S., Dessler, A. E., Dunkerton, T. J., Folkins, I., Fu, Q., and Mote, P. W.: Tropical Tropopause Layer, *Rev. Geophys.*, 47, RG1004, doi:10.1029/2008rg000267, 2009. 12501
- Holtstlag, A. and Boville, B.: Local versus nonlocal boundary-layer diffusion in a global climate model, *J. Climate*, 6, 1825–1842, 1993. 12490
- Hossaini, R., Chipperfield, M. P., Monge-Sanz, B. M., Richards, N. A. D., Atlas, E., and Blake, D. R.: Bromoform and dibromomethane in the tropics: a 3-D model study of chemistry

**Evaluating
emissions of
biogenic
bromocarbons**

R. Hossaini et al.

Title Page

Abstract

Introduction

Conclusions

References

Tables

Figures

◀

▶

◀

▶

Back

Close

Full Screen / Esc

Printer-friendly Version

Interactive Discussion

and transport, *Atmos. Chem. Phys.*, 10, 719–735, doi:10.5194/acp-10-719-2010, 2010. 12506

Hossaini, R., Chipperfield, M. P., Dhomse, S., Ordonez, C., Saiz-Lopez, A., Abraham, N. L., Archibald, A., Braesicke, P., Telford, P., Warwick, N., Yang, X., and Pyle, J.: Modelling future changes to the stratospheric source gas injection of biogenic bromocarbons, *Geophys. Res. Lett.*, 39, L20813, doi:10.1029/2012gl053401, 2012a. 12489, 12508

Hossaini, R., Chipperfield, M. P., Feng, W., Breider, T. J., Atlas, E., Montzka, S. A., Miller, B. R., Moore, F., and Elkins, J.: The contribution of natural and anthropogenic very short-lived species to stratospheric bromine, *Atmos. Chem. Phys.*, 12, 371–380, doi:10.5194/acp-12-371-2012, 2012b. 12489, 12490, 12493, 12506, 12507

Kreygy, S., Camy-Peyret, C., Chipperfield, M. P., Dorf, M., Feng, W., Hossaini, R., Kritten, L., Werner, B., and Pfeilsticker, K.: Atmospheric test of the $J(\text{BrONO}_2)/k_{\text{BrO}+\text{NO}_2}$ ratio: implications for total stratospheric Br_y and bromine-mediated ozone loss, *Atmos. Chem. Phys. Discuss.*, 12, 27821–27845, doi:10.5194/acpd-12-27821-2012, 2012. 12508

Krüger, K. and Quack, B.: Introduction to special issue: the *TransBrom Sonne* expedition in the tropical West Pacific, *Atmos. Chem. Phys. Discuss.*, 12, 1401–1418, doi:10.5194/acpd-12-1401-2012, 2012. 12502, 12505

Krüger, K., Tegtmeier, S., and Rex, M.: Variability of residence time in the Tropical Tropopause Layer during Northern Hemisphere winter, *Atmos. Chem. Phys.*, 9, 6717–6725, doi:10.5194/acp-9-6717-2009, 2009. 12501

Lary, D.: Gas phase atmospheric bromine photochemistry, *J. Geophys. Res.-Atmos.*, 101, 1505–1516, doi:10.1029/95jd02463, 1996. 12488

Lary, D. and Toumi, R.: Halogen-catalyzed methane oxidation, *J. Geophys. Res.-Atmos.*, 102, 23421–23428, doi:10.1029/97jd00914, 1997. 12488

Leedham, E. C., Hughes, C., Keng, F. S. L., Phang, S.-M., Malin, G., and Sturges, W. T.: Emission of atmospherically significant halocarbons by naturally occurring and farmed tropical macroalgae, *Biogeosciences Discuss.*, 10, 483–528, doi:10.5194/bgd-10-483-2013, 2013. 12502, 12504

Levine, J. G., Braesicke, P., Harris, N. R. P., Savage, N. H., and Pyle, J. A.: Pathways and timescales for troposphere-to-stratosphere transport via the tropical tropopause layer and their relevance for very short lived substances, *J. Geophys. Res.-Atmos.*, 112, D04308, doi:10.1029/2005jd006940, 2007. 12502

**Evaluating
emissions of
biogenic
bromocarbons**

R. Hossaini et al.

Title Page

Abstract

Introduction

Conclusions

References

Tables

Figures

◀

▶

◀

▶

Back

Close

Full Screen / Esc

Printer-friendly Version

Interactive Discussion

- Liang, Q., Stolarski, R. S., Kawa, S. R., Nielsen, J. E., Douglass, A. R., Rodriguez, J. M., Blake, D. R., Atlas, E. L., and Ott, L. E.: Finding the missing stratospheric Br_y : a global modeling study of CHBr_3 and CH_2Br_2 , *Atmos. Chem. Phys.*, 10, 2269–2286, doi:10.5194/acp-10-2269-2010, 2010. 12491, 12493, 12502, 12509, 12510
- 5 Montzka, S., Butler, J., Hall, B., Mondeel, D., and Elkins, J.: A decline in tropospheric organic bromine, *Geophys. Res. Lett.*, 30, 1826, doi:10.1029/2003gl017745, 2003. 12489, 12494
- Montzka, S., Reimann, S., Engel, A., Krüger, K., O'Doherty, S., Sturges, W. T., Blake, D., Dorf, M., Fraser, P., Froidevaux, L., Jucks, K., Kreher, K., Kurylo, M. J., Mellouki, A., Miller, J., Nielsen, O.-J., Orkin, V. L., Prinn, R. G., Rzew, R., Santee, M. L., Stohl, A., and Verdonik, D.:
10 Ozone-Depleting Substances (ODSS) and related chemicals, in: Scientific Assessment of Ozone Depletion: 2010, Global Ozone Research and Monitoring Project, Report No. 52, Chapt. 1, World Meteorological Organization, Geneva, 2011 12489, 12493, 12496
- Ordóñez, C., Lamarque, J.-F., Tilmes, S., Kinnison, D. E., Atlas, E. L., Blake, D. R., Sousa Santos, G., Brasseur, G., and Saiz-Lopez, A.: Bromine and iodine chemistry in a global chemistry-climate model: description and evaluation of very short-lived oceanic sources, *Atmos. Chem. Phys.*, 12, 1423–1447, doi:10.5194/acp-12-1423-2012, 2012. 12491, 12493,
15 12502, 12509
- Patra, P. K., Houweling, S., Krol, M., Bousquet, P., Belikov, D., Bergmann, D., Bian, H., Cameron-Smith, P., Chipperfield, M. P., Corbin, K., Fortems-Cheiney, A., Fraser, A., Gloor, E., Hess, P., Ito, A., Kawa, S. R., Law, R. M., Loh, Z., Maksyutov, S., Meng, L., Palmer, P. I.,
20 Prinn, R. G., Rigby, M., Saito, R., and Wilson, C.: TransCom model simulations of CH_4 and related species: linking transport, surface flux and chemical loss with CH_4 variability in the troposphere and lower stratosphere, *Atmos. Chem. Phys.*, 11, 12813–12837, doi:10.5194/acp-11-12813-2011, 2011. 12511
- 25 Pfeilsticker, K., Sturges, W., Bosch, H., Camy-Peyret, C., Chipperfield, M., Engel, A., Fitzenberger, R., Müller, M., Payan, S., and Sinnhuber, B.: Lower stratospheric organic and inorganic bromine budget for the Arctic winter 1998/99, *Geophys. Res. Lett.*, 27, 3305–3308, doi:10.1029/2000gl011650, 2000. 12489
- Pfeilsticker, K. and the SHIVA consortium: Overview on the project SHIVA (Stratospheric ozone: halogen impacts in a varying atmosphere): achievements and key results, in preparation,
30 2013. 12503
- Prather, M.: Numerical advection by conservation of 2nd-order moments, *J. Geophys. Res.-Atmos.*, 91, 6671–6681, doi:10.1029/jd091id06p06671, 1986. 12490

**Evaluating
emissions of
biogenic
bromocarbons**

R. Hossaini et al.

Title Page

Abstract

Introduction

Conclusions

References

Tables

Figures

◀

▶

◀

▶

Back

Close

Full Screen / Esc

Printer-friendly Version

Interactive Discussion

- Pyle, J. A., Ashfold, M. J., Harris, N. R. P., Robinson, A. D., Warwick, N. J., Carver, G. D., Gostlow, B., O'Brien, L. M., Manning, A. J., Phang, S. M., Yong, S. E., Leong, K. P., Ung, E. H., and Ong, S.: Bromoform in the tropical boundary layer of the Maritime Continent during OP3, *Atmos. Chem. Phys.*, 11, 529–542, doi:10.5194/acp-11-529-2011, 2011. 12491, 12502
- 5 Quack, B. and Wallace, D.: Air-sea flux of bromoform: controls, rates, and implications, *Global Biogeochem. Cy.*, 17, 1023, doi:10.1029/2002gb001890, 2003. 12488
- Read, K. A., Mahajan, A. S., Carpenter, L. J., Evans, M. J., Faria, B. V. E., Heard, D. E., Hopkins, J. R., Lee, J. D., Moller, S. J., Lewis, A. C., Mendes, L., Mcquaid, J. B., Oetjen, H., Saiz-Lopez, A., Pilling, M. J., and Plane, J. M. C.: Extensive halogen-mediated ozone destruction
10 over the tropical Atlantic Ocean, *Nature*, 453, 1232–1235, doi:10.1038/Nature07035, 2008. 12488
- Saiz-Lopez, A. and Von Glasow, R.: Reactive halogen chemistry in the troposphere, *Chem. Soc. Rev.*, 41, 6448–6472, doi:10.1039/c2cs35208g, 2012. 12488
- Saiz-Lopez, A., Lamarque, J.-F., Kinnison, D. E., Tilmes, S., Ordóñez, C., Orlando, J. J., Con-
15 ley, A. J., Plane, J. M. C., Mahajan, A. S., Sousa Santos, G., Atlas, E. L., Blake, D. R., Sander, S. P., Schauffler, S., Thompson, A. M., and Brasseur, G.: Estimating the climate significance of halogen-driven ozone loss in the tropical marine troposphere, *Atmos. Chem. Phys.*, 12, 3939–3949, doi:10.5194/acp-12-3939-2012, 2012. 12488
- Sala, S., Bönisch, H., Keber, T., and Engel, A.: A budget of total organic bromine from airborne
20 vsls measurements during shiva, in preparation, 2013. 12503, 12504, 12537
- Salawitch, R., Weisenstein, D., Kovalenko, L., Sioris, C., Wennberg, P., Chance, K., Ko, M., and McLinden, C.: Sensitivity of ozone to bromine in the lower stratosphere, *Geophys. Res. Lett.*,
32, L05811, doi:10.1029/2004gl021504, 2005. 12488
- Salawitch, R. J., Canty, T., Kurosu, T., Chance, K., Liang, Q., Da Silva, A., Pawson, S.,
25 Nielsen, J. E., Rodriguez, J. M., Bhartia, P. K., Liu, X., Huey, L. G., Liao, J., Stickel, R. E., Tanner, D. J., Dibb, J. E., Simpson, W. R., Donohoue, D., Weinheimer, A., Flocke, F., Knapp, D., Montzka, D., Neuman, J. A., Nowak, J. B., Ryerson, T. B., Oltmans, S., Blake, D. R., Atlas, E. L., Kinnison, D. E., Tilmes, S., Pan, L. L., Hendrick, F., Van Roozendaal, M., Kreher, K., Johnston, P. V., Gao, R. S., Johnson, B., Bui, T. P., Chen, G., Pierce, R. B., Crawford, J. H.,
30 and Jacob, D. J.: A new interpretation of total column bro during arctic spring, *Geophys. Res. Lett.*, 37, L21805, doi:10.1029/2010gl043798, 2010. 12489, 12511
- Sander, S., Friedl, R., Barker, J., Golden, D., Kurylo, M., Wine, P., Abbatt, J., Burkholder, J., Kolb, C., Moortgat, G., Huie, R., and Orkin, V.: Chemical Kinetics and Photochemical Data

**Evaluating
emissions of
biogenic
bromocarbons**

R. Hossaini et al.

Title Page

Abstract

Introduction

Conclusions

References

Tables

Figures

◀

▶

◀

▶

Back

Close

Full Screen / Esc

Printer-friendly Version

Interactive Discussion

for Use in Atmospheric Studies, Evaluation Number 17, JPL Publication 10-6, Jet Propulsion Laboratory, 2011. 12491

Schofield, R., Fueglistaler, S., Wohltmann, I., and Rex, M.: Sensitivity of stratospheric Br_y to uncertainties in very short lived substance emissions and atmospheric transport, *Atmos. Chem. Phys.*, 11, 1379–1392, doi:10.5194/acp-11-1379-2011, 2011. 12489

Sioris, C. E., Kovalenko, L. J., McLinden, C. A., Salawitch, R. J., Van Roozendaal, M., Goutail, F., Dorf, M., Pfeilsticker, K., Chance, K., von Savigny, C., Liu, X., Kurosu, T. P., Pomereau, J. P., Boesch, H., and Frerick, J.: Latitudinal and vertical distribution of bromine monoxide in the lower stratosphere from Scanning imaging absorption spectrometer for atmospheric cartography limb scattering measurements, *J. Geophys. Res.-Atmos.*, 111, D14301, doi:10.1029/2005jd006479, 2006. 12489

Solomon, S.: Stratospheric ozone depletion: a review of concepts and history, *Rev. Geophys.*, 37, 275–316, 1999. 12488

Stockwell, D. and Chipperfield, M.: A tropospheric chemical-transport model: development and validation of the model transport schemes, *Q. J. Roy. Meteor. Soc.*, 125, 1747–1783, doi:10.1256/Smsqj.55713, 1999. 12490

Sturges, W., Oram, D., Carpenter, L., Penkett, S., and Engel, A.: Bromoform as a source of stratospheric bromine, *Geophys. Res. Lett.*, 27, 2081–2084, doi:10.1029/2000gl011444, 2000. 12489

Swanson, A., Davis, D., Arimoto, R., Robert, P., Atlas, E., Flocke, F., Meinardi, S., Rowland, F., and Blake, D.: Organic trace gases of oceanic origin observed at south pole during ISCAT 2000, *Atmos. Environ.*, 38, 5463–5472, doi:10.1016/J.Atmosenv.2004.03.072, 2004. 12496

Tegtmeier, S., Krüger, K., Quack, B., Atlas, E. L., Pisso, I., Stohl, A., and Yang, X.: Emission and transport of bromocarbons: from the West Pacific ocean into the stratosphere, *Atmos. Chem. Phys.*, 12, 10633–10648, doi:10.5194/acp-12-10633-2012, 2012. 12489

Tiedtke, M.: A comprehensive mass flux scheme for cumulus parameterization in large-scale models, *Mon. Wea. Rev.*, 117, 1779–1800, doi:10.1175/1520-0493, 1989. 12490

von Glasow, R., von Kuhlmann, R., Lawrence, M. G., Platt, U., and Crutzen, P. J.: Impact of reactive bromine chemistry in the troposphere, *Atmos. Chem. Phys.*, 4, 2481–2497, doi:10.5194/acp-4-2481-2004, 2004. 12488

Warwick, N. J., Pyle, J. A., Carver, G. D., Yang, X., Savage, N. H., O'Connor, F. M., and Cox, R. A.: Global modeling of biogenic bromocarbons, *J. Geophys. Res.-Atmos.*, 111, D24305, doi:10.1029/2006jd007264, 2006. 12491, 12493

Evaluating emissions of biogenic bromocarbons

R. Hossaini et al.

Title Page

Abstract

Introduction

Conclusions

References

Tables

Figures

◀

▶

◀

▶

Back

Close

Full Screen / Esc

Printer-friendly Version

Interactive Discussion

WMO: Scientific Assessment of Ozone Depletion: 2006, Global Ozone Research and Monitoring Project, Report No. 50, World Meteorological Organization, Geneva, Switzerland, 2007. 12508

WMO: Scientific Assessment of Ozone Depletion: 2010, Global Ozone Research and Monitoring Project, Report No. 52, World Meteorological Organization, Geneva, Switzerland, 2011. 12488, 12506, 12508, 12511

Wofsy, S. C., Team, H. S., Team, C. M., and Team, S.: HIAPER Pole-To-Pole Observations (HIPPO): fine-grained, global-scale measurements of climatically important atmospheric gases and aerosols, *Philos. T. Roy. Soc. A*, 369, 2073–2086, doi:10.1098/Rsta.2010.0313, 2011. 12499

Worton, D. R., Mills, G. P., Oram, D. E., and Sturges, W. T.: Gas chromatography negative ion chemical ionization mass spectrometry: application to the detection of alkyl nitrates and halocarbons in the atmosphere, *J. Chromatogr. A*, 1201, 112–119, doi:10.1016/J.Chroma.2008.06.019, 2008. 12503

Yang, X., Cox, R., Warwick, N., Pyle, J., Carver, G., O'connor, F., and Savage, N.: Tropospheric bromine chemistry and its impacts on ozone: a model study, *J. Geophys. Res.-Atmos.*, 110, D23311, doi:10.1029/2005jd006244, 2005. 12488

Yokouchi, Y., Barrie, L., Toom, D., and Akimoto, H.: The seasonal variation of selected natural and anthropogenic halocarbons in the Arctic Troposphere, *Atmos. Environ.*, 30, 1723–1727, doi:10.1016/1352-2310(95)00393-2, 1996. 12495

Ziska, F., Quack, B., Abrahamsson, K., Archer, S. D., Atlas, E., Bell, T., Butler, J. H., Carpenter, L. J., Jones, C. E., Harris, N. R. P., Hepach, H., Heumann, K. G., Hughes, C., Kuss, J., Krüger, K., Liss, P., Moore, R. M., Orlikowska, A., Raimund, S., Reeves, C. E., Reifenhäuser, W., Robinson, A. D., Schall, C., Tanhua, T., Tegtmeier, S., Turner, S., Wang, L., Wallace, D., Williams, J., Yamamoto, H., Yvon-Lewis, S., and Yokouchi, Y.: Global sea-to-air flux climatology for bromoform, dibromomethane and methyl iodide, *Atmos. Chem. Phys. Discuss.*, 13, 5601–5648, doi:10.5194/acpd-13-5601-2013, 2013. 12491, 12492, 12493, 12505, 12509, 12510

Evaluating emissions of biogenic bromocarbons

R. Hossaini et al.

Table 1. Summary of 14 yr CTM runs and the global total source strength (Gg source gas yr⁻¹) of CHBr₃ and CH₂Br₂.

Run	Scenario	Derivation	CHBr ₃	CH ₂ Br ₂
<i>S</i> _{Liang}	Liang-2010	Top-down	450	62
<i>S</i> _{Warwick}	Warwick-2011	Top-down	380	113
<i>S</i> _{Ordonez}	Ordóñez-2012	Top-down	533	67
<i>S</i> _{Ziska}	Ziska-2013	Bottom-up	183	64

Title Page

Abstract

Introduction

Conclusions

References

Tables

Figures

◀

▶

◀

▶

Back

Close

Full Screen / Esc

Printer-friendly Version

Interactive Discussion

Evaluating emissions of biogenic bromocarbons

R. Hossaini et al.

Title Page

Abstract

Introduction

Conclusions

References

Tables

Figures

⏪

⏩

◀

▶

Back

Close

Full Screen / Esc

Printer-friendly Version

Interactive Discussion



Table 2. Summary and location of NOAA/ESRL ground-based stations arranged from north to south.

Station	Name	Lat	Lon
ALT	Alert, NW Territories, Canada	82.5° N	62.3° W
SUM*	Summit, Greenland	72.6° N	38.4° W
BRW	Pt. Barrow, Alaska, USA	71.3° N	156.6° W
MHD	Mace Head, Ireland	53.0° N	10.0° W
LEF	Wisconsin, USA	45.6° N	90.2° W
HFM	Massachusetts, USA	42.5° N	72.2° W
THD	Trinidad Head, USA	41.0° N	124.0° W
NWR	Niwot Ridge, Colorado, USA	40.1° N	105.6° W
KUM	Cape Kumukahi, Hawaii, USA	19.5° N	154.8° W
MLO*	Mauna Loa, Hawaii, USA	19.5° N	155.6° W
SMO	Cape Matatula, American Samoa	14.3° S	170.6° W
CGO	Cape Grim, Tasmania, Australia	40.7° S	144.8° E
PSA	Palmer Station, Antarctica	64.6° S	64.0° W
SPO*	South Pole	90.0° S	–

* Stations SUM, MLO and SPO elevated at ~ 3210 m, 3397 m and 2810 m, respectively.

Evaluating emissions of biogenic bromocarbons

R. Hossaini et al.

Table 4. As Table 3 but for CH₂Br₂.

Latitude	Run S _{Liang}			Run S _{Warwick}			Run S _{Ordonez}			Run S _{Ziska}		
	MB	MAD	MAPE	MB	MAD	MAPE	MB	MAD	MAPE	MB	MAD	MAPE
≥ 60° N	-0.11	0.15	15 %	0.08	0.14	16 %	-0.11	0.15	15 %	-0.34	0.36	36 %
30–60° N	-0.03	0.28	27 %	0.18	0.33	37 %	-0.00	0.24	24 %	0.02	0.21	22 %
±30°	0.14	0.17	24 %	1.25	1.25	167 %	0.35	0.35	49 %	0.63	0.63	85 %
30–60° S	-0.05	0.10	10 %	0.47	0.49	48 %	-0.25	0.25	23 %	0.93	0.94	92 %
≥ 60° S	-0.11	0.12	13 %	0.43	0.45	55 %	-0.19	0.19	21 %	1.14	1.14	137 %
Global	-0.02	0.19	20 %	0.44	0.52	64 %	0.00	0.24	27 %	0.30	0.52	60 %

Title Page

Abstract

Introduction

Conclusions

References

Tables

Figures

⏪

⏩

◀

▶

Back

Close

Full Screen / Esc

Printer-friendly Version

Interactive Discussion

Evaluating emissions of biogenic bromocarbons

R. Hossaini et al.

Table 5. Summary of calculated error metrics between CHBr_3 observed in the free troposphere during the HIPPO project (2009–2011) and with analogous fields from CTM runs S_{Liang} , S_{Warwick} , S_{Ordonez} and S_{Ziska} . Shown is the mean bias (MB) and the mean absolute deviation (MAD) both in units of ppt. Also shown is the mean absolute percentage error (MAPE, see text). These fields were calculated for all observations made during HIPPO missions 1–5 for the 5 latitudinal bands shown in Fig. 4. A global value is also quoted for comparisons at all latitudes.

Latitude	Run S_{Liang}			Run S_{Warwick}			Run S_{Ordonez}			Run S_{Ziska}		
	MB	MAD	MAPE	MB	MAD	MAPE	MB	MAD	MAPE	MB	MAD	MAPE
$\geq 60^\circ \text{ N}$	-0.16	0.23	31%	-0.55	0.55	63%	-0.03	0.24	37%	-0.25	0.26	38%
$30\text{--}60^\circ \text{ N}$	0.04	0.12	28%	-0.27	0.29	42%	0.22	0.23	51%	-0.25	0.25	42%
$\pm 30^\circ$	0.30	0.31	63%	0.32	0.33	68%	0.51	0.51	102%	-0.19	0.20	35%
$30\text{--}60^\circ \text{ S}$	0.09	0.13	45%	-0.07	0.13	39%	0.19	0.21	69%	-0.18	0.19	42%
$\geq 60^\circ \text{ S}$	-0.12	0.21	42%	-0.37	0.40	60%	0.06	0.28	62%	-0.40	0.41	54%
Global	0.04	0.20	42%	-0.17	0.34	54%	0.21	0.30	65%	-0.24	0.25	41%

[Title Page](#)
[Abstract](#)
[Introduction](#)
[Conclusions](#)
[References](#)
[Tables](#)
[Figures](#)
[Back](#)
[Close](#)
[Full Screen / Esc](#)
[Printer-friendly Version](#)
[Interactive Discussion](#)

Evaluating emissions of biogenic bromocarbons

R. Hossaini et al.

Table 6. As Table 5 but for CH₂Br₂.

Latitude	Run S _{Liang}			Run S _{Warwick}			Run S _{Ordonez}			Run S _{Ziska}		
	MB	MAD	MAPE	MB	MAD	MAPE	MB	MAD	MAPE	MB	MAD	MAPE
≥ 60° N	-0.10	0.17	23 %	0.25	0.29	57 %	-0.02	0.16	24 %	-0.12	0.28	39 %
30–60° N	-0.02	0.15	19 %	0.47	0.47	75 %	0.08	0.17	25 %	0.11	0.25	37 %
±30°	0.12	0.13	16 %	1.11	1.11	134 %	0.24	0.24	29 %	0.54	0.54	66 %
30–60° S	-0.01	0.09	13 %	0.67	0.67	101 %	0.01	0.12	18 %	0.55	0.55	77 %
≥ 60° S	-0.09	0.13	18 %	0.43	0.43	69 %	-0.06	0.17	23 %	0.55	0.73	96 %
Global	-0.01	0.13	18 %	0.60	0.61	88 %	0.06	0.17	24 %	0.30	0.45	60 %

Title Page

Abstract

Introduction

Conclusions

References

Tables

Figures

⏪

⏩

◀

▶

Back

Close

Full Screen / Esc

Printer-friendly Version

Interactive Discussion

Evaluating emissions of biogenic bromocarbons

R. Hossaini et al.

Table 7. Summary of calculated error metrics between CHBr₃ observed in the free troposphere during 14 flights of the SHIVA aircraft campaign (November–December 2011) and with analogous fields from CTM runs S_{Liang} , S_{Warwick} , S_{Ordonez} and S_{Ziska} . Shown is the mean bias (MB) and the mean absolute deviation (MAD) both in units of ppt. Also shown is the mean absolute percentage error (MAPE, see text). These fields were calculated for all observations from both instruments deployed during SHIVA (i.e. GhOST-MS and WASP, see text). A mean value for all 14 flights is also reported.

Flight	Run S_{Liang}			Run S_{Warwick}			Run S_{Ordonez}			Run S_{Ziska}		
	MB	MAD	MAPE	MB	MAD	MAPE	MB	MAD	MAPE	MB	MAD	MAPE
1a	1.75	1.75	222 %	0.88	0.88	117 %	1.69	1.69	216 %	0.38	0.44	57 %
1b	0.65	0.65	130 %	0.51	0.51	103 %	0.77	0.77	154 %	-0.02	0.12	20 %
2	0.66	0.74	52 %	-0.07	0.33	23 %	0.72	0.76	56 %	0.51	0.69	46 %
3	0.79	0.79	101 %	0.32	0.37	54 %	0.94	0.94	122 %	0.21	0.30	38 %
4	0.57	0.64	87 %	0.17	0.42	62 %	0.71	0.76	102 %	-0.64	0.69	45 %
5a	0.53	0.61	150 %	0.27	0.44	103 %	0.58	0.63	154 %	-0.19	0.28	37 %
5b	1.28	1.31	223 %	0.65	0.73	129 %	1.24	1.27	215 %	0.09	0.33	45 %
6	1.31	1.31	348 %	0.79	0.79	215 %	1.26	1.26	334 %	0.15	0.17	45 %
7b	0.88	0.88	146 %	0.40	0.41	78 %	0.92	0.92	155 %	0.02	0.18	29 %
8	0.69	0.70	122 %	0.46	0.48	88 %	0.83	0.83	143 %	-0.08	0.21	29 %
9a	1.10	1.10	192 %	0.50	0.50	102 %	1.13	1.13	198 %	0.30	0.35	56 %
9b	1.05	1.05	216 %	0.55	0.57	138 %	1.08	1.08	224 %	0.17	0.27	49 %
10a	0.58	0.66	105 %	0.10	0.45	63 %	0.78	0.83	123 %	-0.37	0.46	36 %
10b	0.64	0.69	108 %	0.14	0.40	60 %	0.84	0.86	128 %	-0.27	0.36	32 %
All	0.88	0.91	146 %	0.37	0.50	87 %	0.96	0.98	156 %	-0.00	0.38	41 %

[Title Page](#)
[Abstract](#)
[Introduction](#)
[Conclusions](#)
[References](#)
[Tables](#)
[Figures](#)
[Back](#)
[Close](#)
[Full Screen / Esc](#)
[Printer-friendly Version](#)
[Interactive Discussion](#)


Evaluating emissions of biogenic bromocarbons

R. Hossaini et al.

Table 8. As Table 7 but for CH₂Br₂.

Flight	Run S _{Liang}			Run S _{Warwick}			Run S _{Ordonez}			Run S _{Ziska}		
	MB	MAD	MAPE	MB	MAD	MAPE	MB	MAD	MAPE	MB	MAD	MAPE
1a	0.34	0.41	42 %	1.18	1.18	123 %	0.41	0.46	48 %	0.57	0.59	61 %
1b	0.09	0.11	12 %	1.11	1.11	118 %	0.21	0.22	24 %	0.44	0.44	47 %
2	0.12	0.19	18 %	1.10	1.10	105 %	0.24	0.27	27 %	0.66	0.66	63 %
3	0.22	0.23	27 %	1.09	1.09	126 %	0.35	0.35	41 %	0.56	0.56	65 %
4	0.04	0.13	12 %	0.93	0.93	89 %	0.16	0.19	19 %	0.23	0.25	25 %
5a	0.09	0.19	22 %	0.98	0.98	114 %	0.17	0.22	26 %	0.34	0.36	44 %
5b	0.41	0.41	50 %	1.36	1.36	162 %	0.47	0.47	57 %	0.66	0.66	79 %
6	0.43	0.43	56 %	1.37	1.37	180 %	0.49	0.49	64 %	0.66	0.66	86 %
7b	0.21	0.21	26 %	1.08	1.08	124 %	0.31	0.31	38 %	0.53	0.53	63 %
8	0.13	0.14	16 %	1.12	1.12	124 %	0.26	0.26	29 %	0.58	0.58	64 %
9a	0.28	0.28	32 %	1.12	1.12	131 %	0.37	0.37	43 %	0.59	0.59	69 %
9b	0.28	0.29	36 %	1.22	1.22	147 %	0.38	0.38	47 %	0.68	0.68	83 %
10a	0.10	0.18	20 %	0.94	0.94	104 %	0.22	0.24	28 %	0.32	0.34	39 %
10b	0.12	0.15	17 %	0.96	0.96	103 %	0.25	0.25	27 %	0.37	0.37	41 %
All	0.19	0.23	26 %	1.09	1.09	121 %	0.30	0.31	36 %	0.50	0.50	57 %

Evaluating
emissions of
biogenic
bromocarbons

R. Hossaini et al.

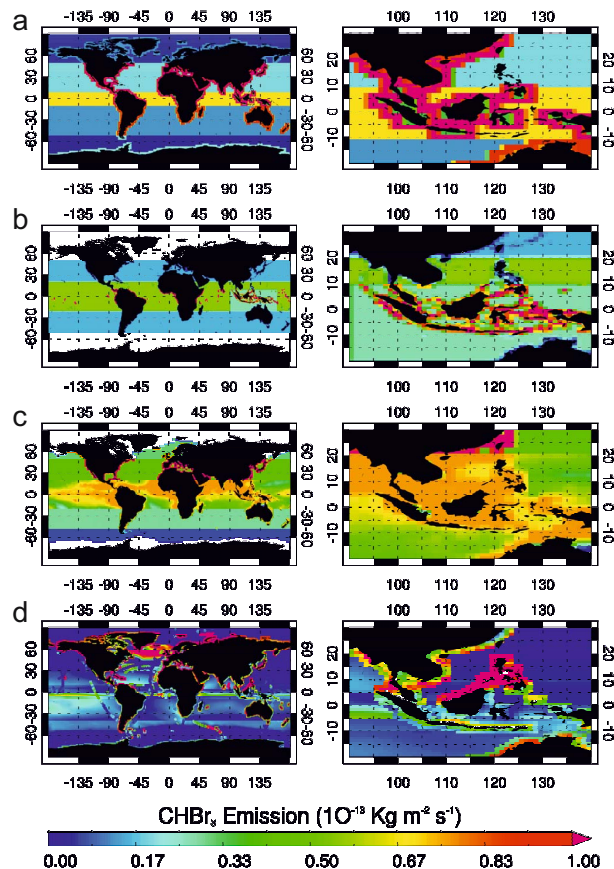


Fig. 1. Bromoform emission field ($10^{-13} \text{ kg m}^{-2} \text{ s}^{-1}$) on $1^\circ \times 1^\circ$ grid for global (left) and Western Pacific (right) regions. Emissions from the (a) Liang-2010, (b) Warwick-2011, (c) Ordóñez-2012 and (d) Ziska-2013 scenarios.

Evaluating
emissions of
biogenic
bromocarbons

R. Hossaini et al.

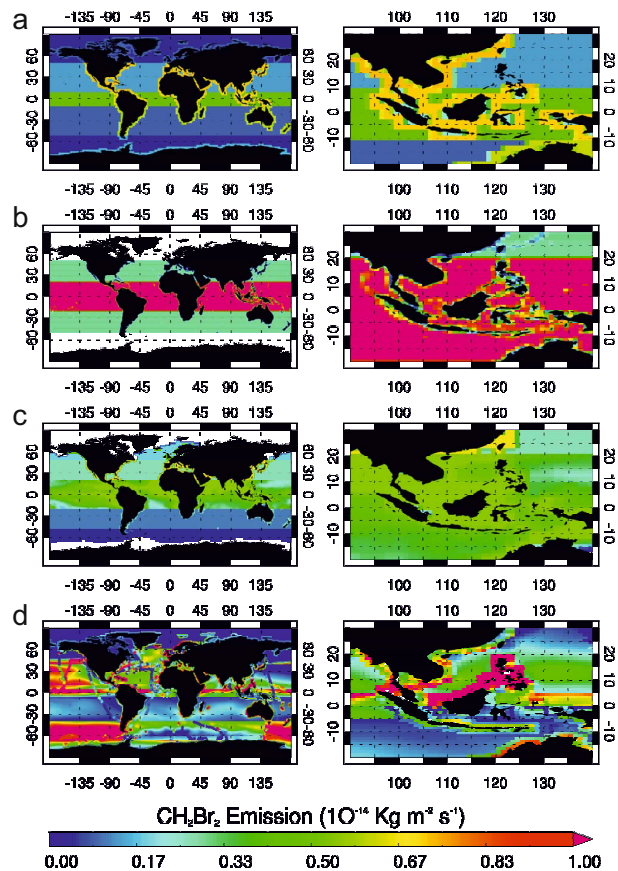


Fig. 2. As Fig. 1 but for dibromomethane ($10^{-14} \text{ kg m}^{-2} \text{ s}^{-1}$). Note the change in scale.

Evaluating
emissions of
biogenic
bromocarbons

R. Hossaini et al.

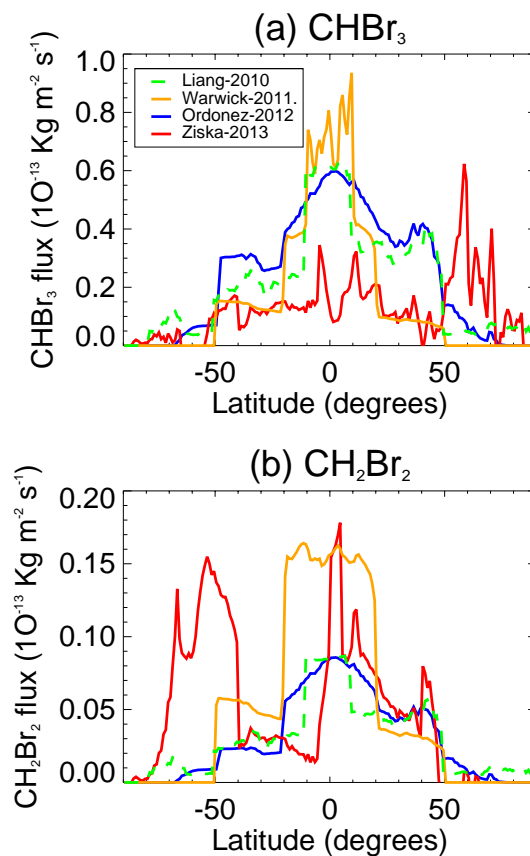


Fig. 3. Zonally averaged global emission source strength ($10^{-13} \text{ kg m}^{-2} \text{ s}^{-1}$) for **(a)** CHBr_3 and **(b)** CH_2Br_2 .

[Title Page](#)[Abstract](#)[Introduction](#)[Conclusions](#)[References](#)[Tables](#)[Figures](#)[◀](#)[▶](#)[◀](#)[▶](#)[Back](#)[Close](#)[Full Screen / Esc](#)[Printer-friendly Version](#)[Interactive Discussion](#)

Evaluating emissions of biogenic bromocarbons

R. Hossaini et al.

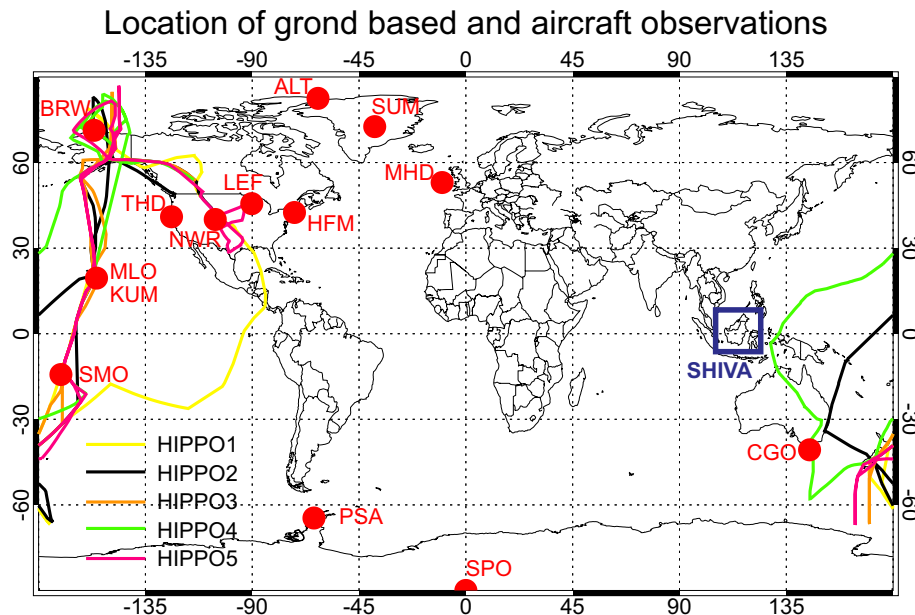


Fig. 4. Location of NOAA/ESRL ground-based monitoring stations. Note, the close proximity of stations MLO and KUM (see Table 2). In this work we group the stations into 5 latitude bands; high NH ($\geq 60^\circ$ N), mid-latitude NH ($30\text{--}60^\circ$ N), tropical ($\pm 30^\circ$), mid-latitude SH ($30\text{--}60^\circ$ S) and high SH ($\geq 60^\circ$ S). Also shown are the flight tracks from the NSF HIPPO aircraft campaigns (1–5) which took place between 2009 and 2011 (see Sect. 4). The location of the SHIVA aircraft campaign (see Sect. 5) that took place in the tropical Western Pacific during November–December 2011 is also indicated.

Title Page

Abstract

Introduction

Conclusions

References

Tables

Figures

◀

▶

◀

▶

Back

Close

Full Screen / Esc

Printer-friendly Version

Interactive Discussion

Evaluating emissions of biogenic bromocarbons

R. Hossaini et al.

Title Page

Abstract

Introduction

Conclusions

References

Tables

Figures

◀

▶

◀

▶

Back

Close

Full Screen / Esc

Printer-friendly Version

Interactive Discussion

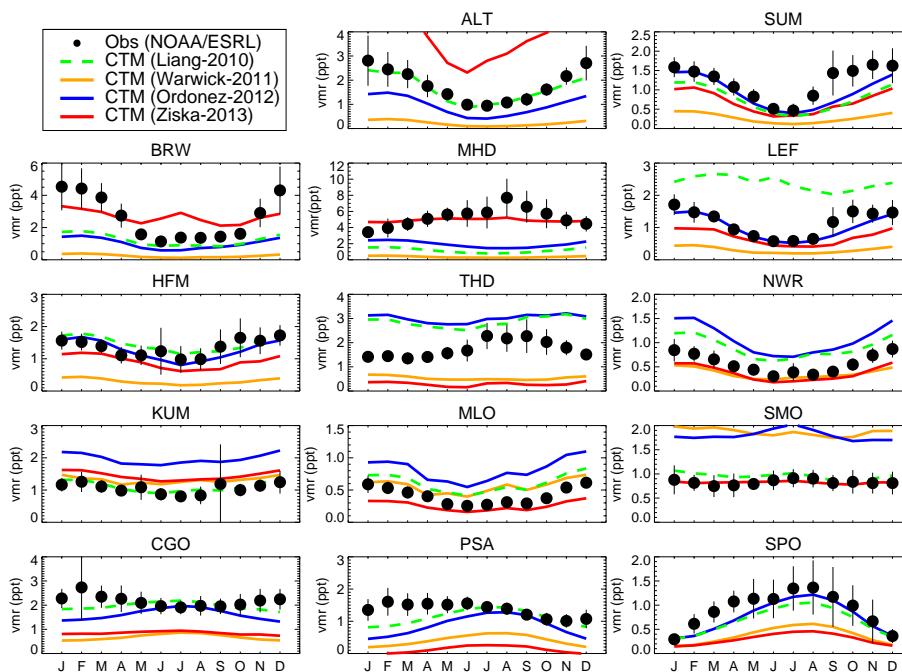


Fig. 5. Comparison of observed monthly mean CHBr_3 mixing ratio (ppt) at 14 NOAA/ESRL ground stations with output from TOMCAT runs S_{Liang} (Liang-2010 emissions), S_{Warwick} (Warwick-2011 emissions), $S_{\text{Ordóñez}}$ (Ordóñez-2012 emissions) and S_{Ziska} (Ziska-2013 emissions). The vertical bars denote ± 1 standard deviation on the observed mean (see text for details).

Evaluating emissions of biogenic bromocarbons

R. Hossaini et al.

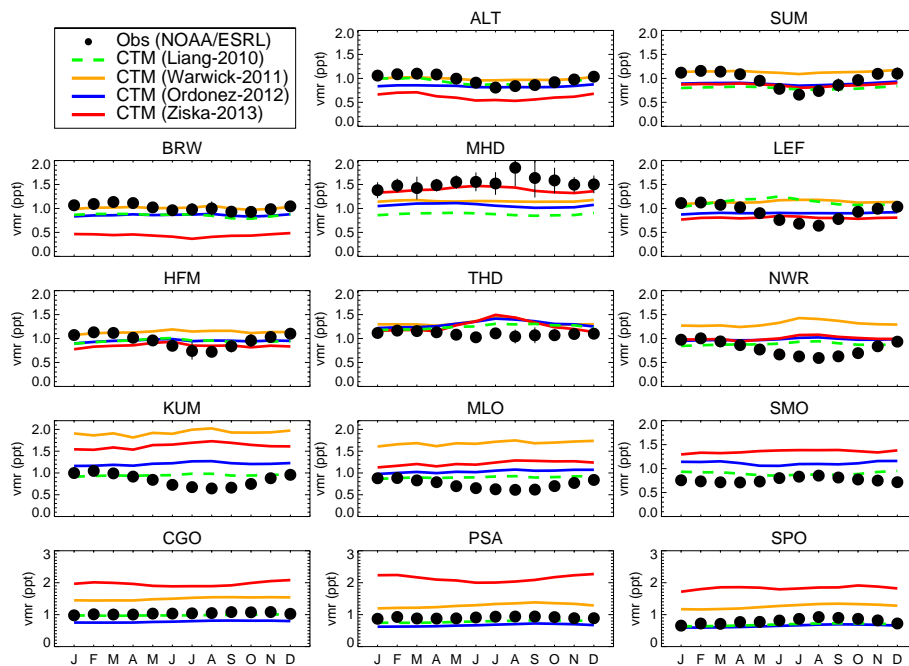


Fig. 6. As Fig. 5 but for CH₂Br₂.

Title Page

Abstract Introduction

Conclusions References

Tables Figures

◀ ▶

◀ ▶

Back Close

Full Screen / Esc

Printer-friendly Version

Interactive Discussion



Evaluating emissions of biogenic bromocarbons

R. Hossaini et al.

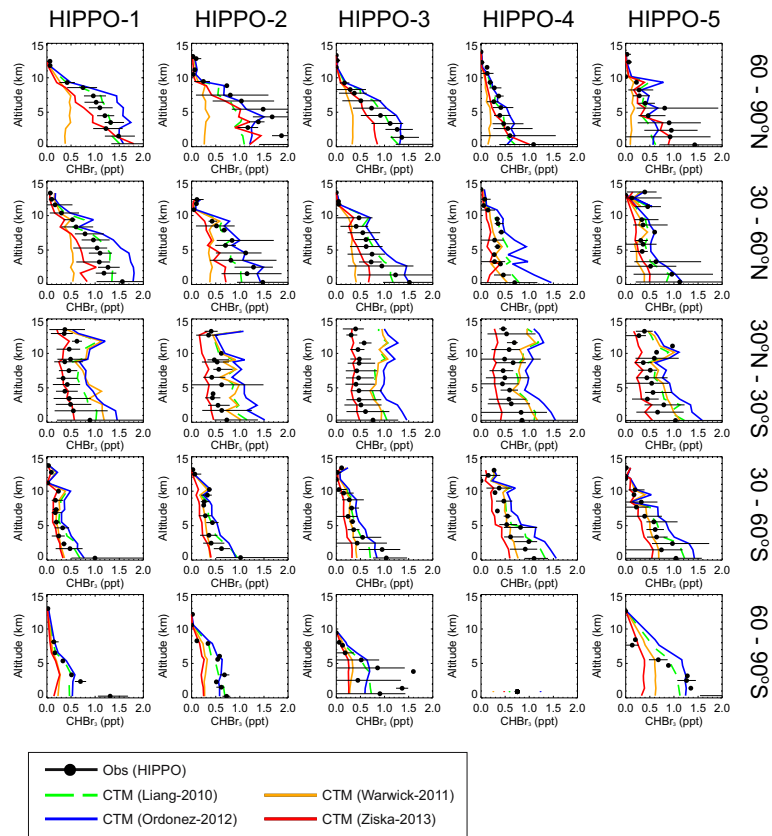


Fig. 7. Comparison of observed CHBr_3 profiles (ppt) made during the NSF HIPPO project (campaigns 1–5, 2009–2011) with analogous modelled profiles from TOMCAT runs S_{Liang} , S_{Warwick} , S_{Ordonez} and S_{Ziska} . All profiles shown are the average for the 5 latitudinal bands considered in this work and are also averaged vertically in ~ 1 km bins. The horizontal lines on the observed data denote the min-max variability from the mean. Note, very few observations were made during HIPPO-4 between 60 and 90° S

Title Page

Abstract Introduction

Conclusions References

Tables Figures

Navigation: Previous, Next, Home, Back, Close

Full Screen / Esc

Printer-friendly Version

Interactive Discussion



Evaluating
emissions of
biogenic
bromocarbons

R. Hossaini et al.

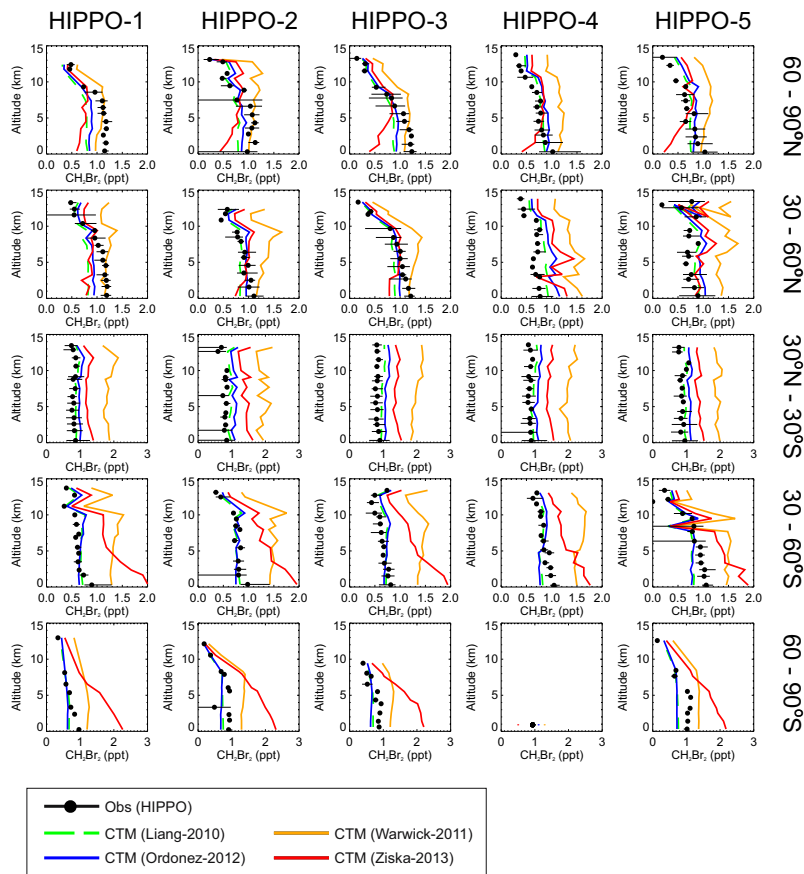


Fig. 8. As Fig. 7 but for CH_2Br_2 .

Title Page

Abstract

Introduction

Conclusions

References

Tables

Figures

◀

▶

◀

▶

Back

Close

Full Screen / Esc

Printer-friendly Version

Interactive Discussion

Evaluating emissions of biogenic bromocarbons

R. Hossaini et al.

Title Page

Abstract

Introduction

Conclusions

References

Tables

Figures

◀

▶

◀

▶

Back

Close

Full Screen / Esc

Printer-friendly Version

Interactive Discussion

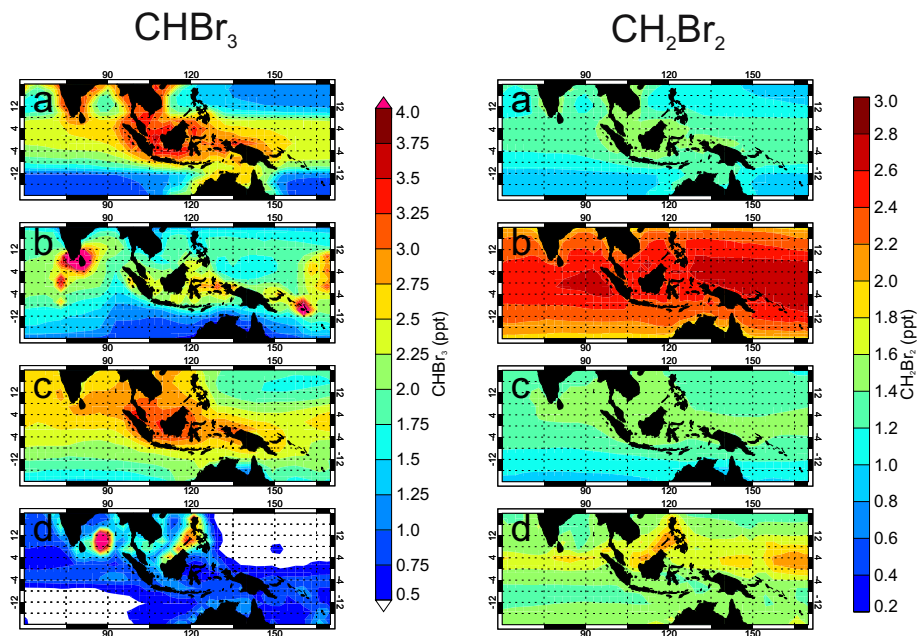


Fig. 9. Modelled mean surface mixing ratio (ppt) of CHBr_3 (left column) and CH_2Br_2 (right column) over the tropical West Pacific during 2011 for CTM runs (a) S_{Liang} , (b) S_{Warwick} , (c) S_{Ordenez} and (d) S_{Ziska} .

Evaluating emissions of biogenic bromocarbons

R. Hossaini et al.

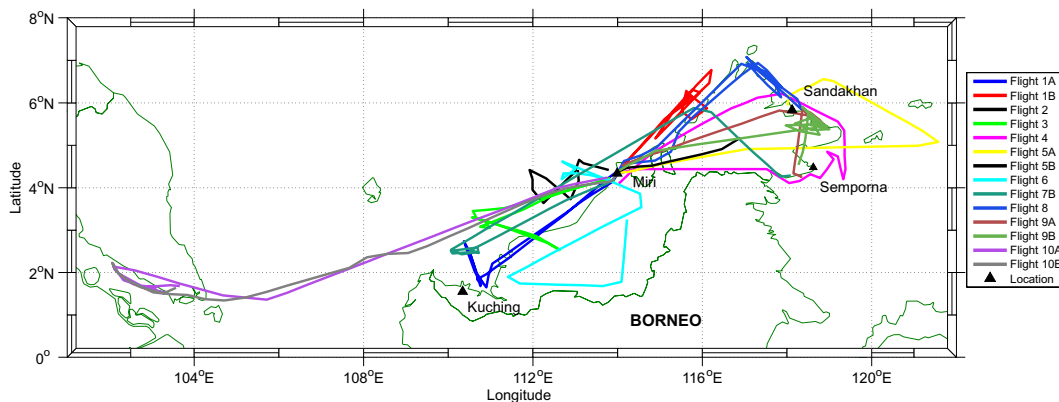


Fig. 10. Flight tracks of the DLR Falcon aircraft during November and December 2011 as part of the 2011 Stratospheric Ozone: Halogen Impacts in a Varying Atmosphere (SHIVA) campaign.

Title Page

Abstract

Introduction

Conclusions

References

Tables

Figures

⏪

⏩

◀

▶

Back

Close

Full Screen / Esc

Printer-friendly Version

Interactive Discussion



Evaluating emissions of biogenic bromocarbons

R. Hossaini et al.

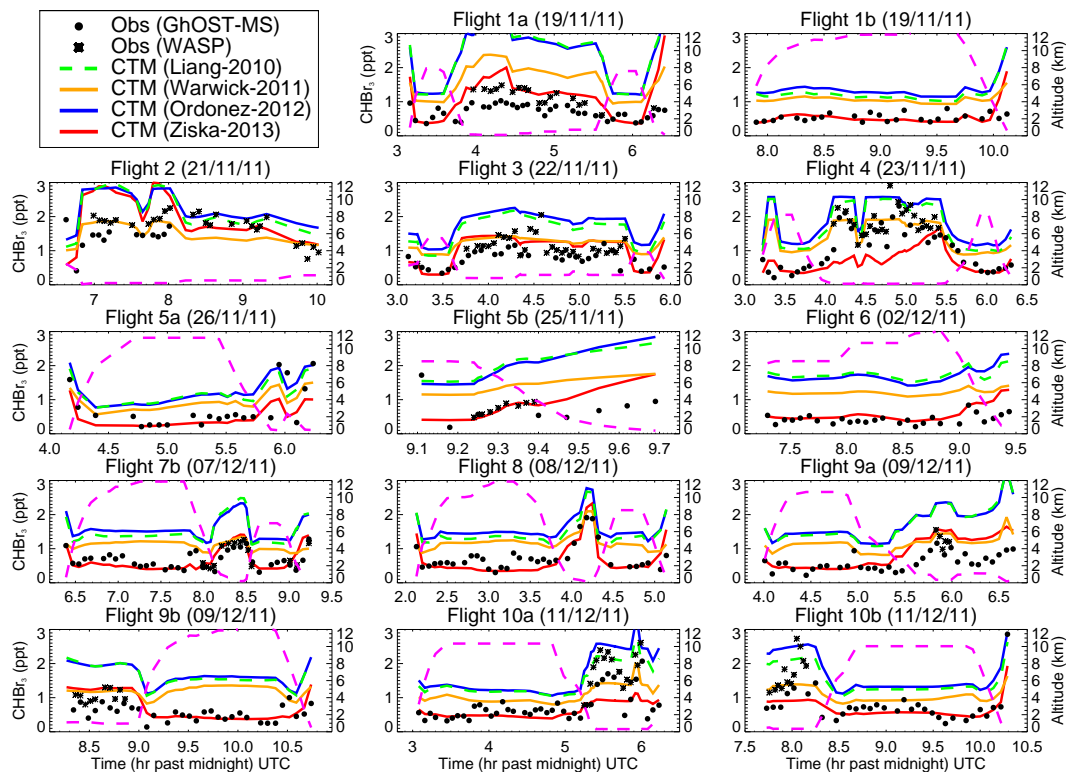
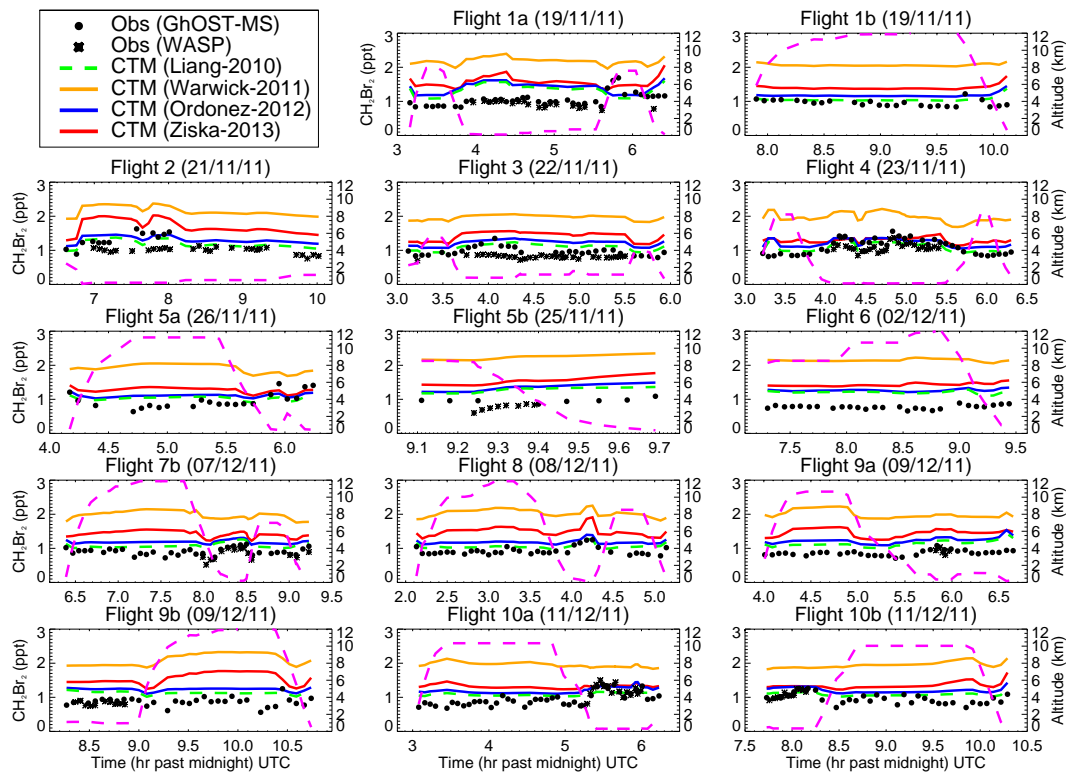


Fig. 11. Comparison between modelled and observed CHBr_3 mixing ratio (ppt) along the flight tracks of the DLR Falcon aircraft during the 2011 SHIVA campaign. Model output is from CTM runs S_{Liang} , S_{Warwick} , S_{Ordonez} and S_{Ziska} and observed data from the GhOST in-situ GC/MS system and the WASP whole air sampler (Sala et al., 2013). The dashed pink line denotes the altitude of the aircraft.

Evaluating emissions of biogenic bromocarbons

R. Hossaini et al.

Fig. 12. As Fig. 11 but for CH_2Br_2 .

Title Page

Abstract

Introduction

Conclusions

References

Tables

Figures



Back

Close

Full Screen / Esc

Printer-friendly Version

Interactive Discussion

Evaluating emissions of biogenic bromocarbons

R. Hossaini et al.

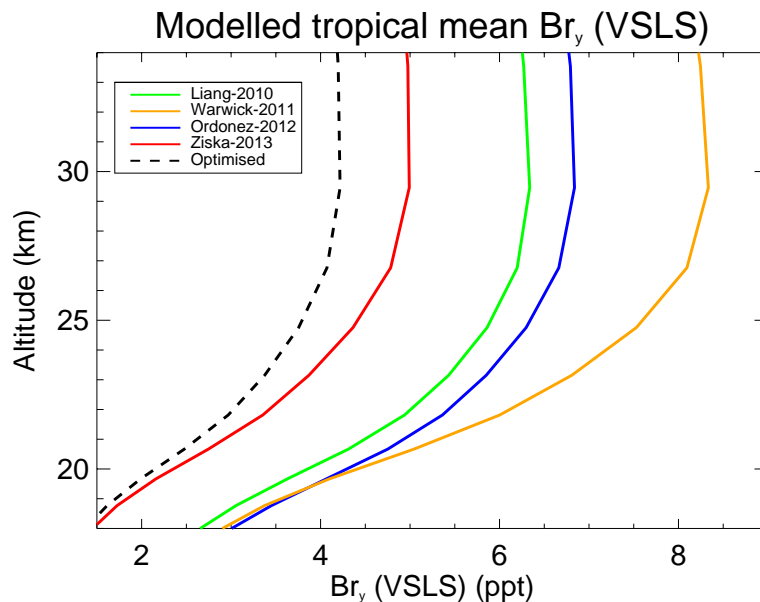


Fig. 13. Modelled 2011 tropical ($\pm 30^\circ$) mean profile of total inorganic bromine (ppt) from CHBr_3 , CH_2Br_2 , CHBr_2Cl , CH_2BrCl and CHBrCl_2 ($\text{Br}_y^{\text{VLSL}}$) in the stratosphere. Profiles are shown for CTM runs S_{Liang} , S_{Warwick} , S_{Ordonez} , and S_{Ziska} . An optimised estimate, calculated by combining CHBr_3 from S_{Ziska} and CH_2Br_2 from S_{Liang} , is also shown.

Title Page

Abstract

Introduction

Conclusions

References

Tables

Figures

⏪

⏩

⏴

⏵

Back

Close

Full Screen / Esc

Printer-friendly Version

Interactive Discussion